SIMULATION AND PERFORMANCE ANALYSIS OF EJECTOR NOZZLE IN A LOW-BYPASS TURBOFAN ENGINE USING NPSS

by

HATIM SOEB RANGWALA

Presented to the Faculty of the Graduate School of

The University of Texas at Arlington in Partial Fulfillment

of the Requirements

for the Degree of

MASTER OF SCIENCE IN AEROSPACE ENGINEERING

THE UNIVERSITY OF TEXAS AT ARLINGTON

MAY 2015

Acknowledgements

First I would like to thank His Holiness, the late Dr. Syedna Mohammad Burhanuddin (TUS) and his successor Syedna Aali Qadr Mufaddal Saiffudin (TUS) for their spiritual guidance without which none of this would be possible.

I would like to thank my thesis advisor Dr. Donald R. Wilson for his invaluable guidance, encouragement and the vast amount of patience he has had with me. I extend my thanks to Dr. Frank Lu and Dr. Brian Dennis for their ideas which shaped my research. Also I would like to thank Mr. Paul Johnson from Wolverine Ventures Inc. (developers of NPSS) for all his technical support regarding NPSS.

I am thankful to my colleagues at the Aerodynamics Research Center: Purushotham Balaji, Vijay Gopal, Warren Frietas and Nanda Kumar for their help and support and, in addition, teaching me the basics of NPSS and helping me through the initial phase of my research.

Finally, I would like to express my deepest gratitude to my parents, Soeb and Jumana Rangwala, my brother and his wife, Mufaddal and Fatema Rangwala for their indispensable support and constant encouragement which made my work much easier.

A special mention of thanks goes to Mrs. Debi Barton of the MAE Department for answering all my queries with patience and for her unconditional support within the department.

April 16, 2015

Abstract

SIMULATION AND PERFORMANCE ANALYSIS OF EJECTOR NOZZLE IN A LOW-BYPASS TURBOFAN ENGINE USING NPSS

Hatim Soeb Rangwala, MS

The University of Texas at Arlington, 2015

Supervising Professor: Donald R. Wilson

Nozzles for propulsive applications in airbreathing engines have long been studied to augment thrust and reduce the size of the engine. They are critical elements of the engine as they convert the internal energy into kinetic energy, thereby producing thrust. Fixed-geometry nozzles are operated optimally only at a particular set of flight conditions and are not efficient at off-design conditions. To improve off-design performance, variable geometry nozzles can be utilized which require complex mechanisms that ultimately increase weight and susceptibility to failure.

Ejector nozzles provide variable geometry capability via aerodynamically varying the effective area ratios of the core and bypass flows. In addition to this, they augment the thrust of the engine by mixing the core and bypass flow, causing an increase in kinetic energy. The increase in kinetic energy is through the exchange of internal energy and momentum of the primary core flow to the secondary bypass flow in a turbofan engine. As most research codes developed by the industry are proprietary, they are not available to academia. That is why a simulation tool called Numerical Propulsion Systems Simulation is used to develop a model of an ejector-nozzle low bypass turbofan engine. A control volume approach is utilized in the formation of the ejector nozzle analytical model.

Using the NPSS model, parametric optimization of bypass ratios at sea-level-static (SLS) conditions is conducted on the ejector-nozzle turbofan engine with the effect

on specific thrust, specific fuel consumption, and nozzle exit area and exit static temperature. The fan and ejector bypass ratios that give optimal performance characteristics are picked for further analysis.

A flight mission envelope is set for the ejector-nozzle turbofan engine that is to be compared with three conventionally configured gas turbine engines: unmixed flow turbofan, mixed flow turbofan and turbojet. At three different flight conditions of supercruise, dash and subsonic cruise, all four configurations are simulated and the performance characteristics of each engine are compared.

The results from this research study should provide a better understanding of ejectors as a thrust augmenting device and is a good starting point for the simulation and performance analysis of ejector nozzles. Concluding the research study, improvements on the ejector-nozzle model developed, are discussed.

Table of Contents

Acknowledgements iii

Abstract iv

List of Illustrations viii

List of Tables x

CHAPTER 1 Introduction 1

1.1 Motivation 1

1.2 Ejector Nozzle 2

1.2.1 Background 2

1.2.2 Thermodynamic Analysis of the Ejector Nozzle 4

1.2.3 Advantages & Disadvantages of Ejector-Nozzle Turbofan Engines 7

CHAPTER 2 Literature Survey 8

CHAPTER 3 Numerical Propulsion System Simulation 11

3.1 Overview 11

3.2 Development of NPSS Code 11

CHAPTER 4 Simulation Setup 17

4.1 Model Flowchart 17

4.2 On-Design 24

4.3 Off-Design 26

4.4 Comparative Models Setup 26

CHAPTER 5 Results 33

5.1 Engine Optimization 33

5.2 Comparative Analysis 42

CHAPTER 6 Conclusion 49

6.1 Summary and Conclusion 49

6.2 Improvements 51

APPENDIX A Results 54

APPENDIX B NPSS Output for Optimized Ejector-Nozzle Turbofan Engine at On-Design Conditions 59

References 76

Biographical Information 79

List of Illustrations

Figure 1-1: Ejector Nozzle Schematic 2

Figure 1-2: Ejector Nozzle Stations 4

Figure 1-3: Temperature-Entropy Diagram for an Ejector Nozzle with Initial Heat Addition to the Primary Flow 5

Figure 3-1: Typical Velocity Distributions in an Ejector Mixing Chamber 16

Figure 4-1: Effect of Alpha on Thrust Augmentation Ratio 20

Figure 4-2: Ejector-nozzle Turbofan Engine Diagram with station numbering 22

Figure 4-3: Ejector-based Turbofan Engine NPSS Element Flowchart 23

Figure 4-4: Unmixed flow Turbofan Engine Diagram 27

Figure 4-5: Mixed flow Turbofan Engine Diagram 28

Figure 4-6: Turbojet Engine Diagram 29

Figure 4-7: Unmixed Flow Low BP Turbofan Engine NPSS Flowchart 30

Figure 4-8: Mixed Flow Low BP Turbofan Engine NPSS Flowchart 31

Figure 4-9: Turbojet Engine NPSS Flowchart 32

Figure 5-1: Variation of SFC as a function of Ejector Bypass Ratio at different Fan Bypass Ratios 34

Figure 5-2: Variation of Combustion Chamber Fuel Flow Rate as a function of Ejector Bypass Ratio at different Fan Bypass Ratios 35

Figure 5-3: Variation of Afterburner Fuel Flow Rate as a function of Ejector Bypass Ratio at different Fan Bypass Ratios 36

Figure 5-4: Variation of Total Fuel Flow Rate as a function of Ejector Bypass Ratio at different Fan Bypass Ratios 37

Figure 5-5: Variation of Mass Flow Rate as a function of Ejector Bypass Ratio at different Fan Bypass Ratios 38

Figure 5-6: Variation of Specific Thrust as a function of Ejector Bypass Ratio at different Fan Bypass Ratios 39
Figure 5-7: Variation of Nozzle Exit Area as a function of Ejector Bypass Ratio at different Fan Bypass Ratios 40
Figure 5-8: Variation of Exit Static Temperature as a function of Ejector Bypass Ratio at different Fan Bypass Ratios 41
Figure 5-9: Mass Flow Rate (Comparative Analysis) 42
Figure 5-10: Combustion Chamber Fuel Flow Rate (Comparative Analysis) 43
Figure 5-11: Afterburner Fuel Flow Rate (Comparative Analysis) 43
Figure 5-12: Gross Thrust (Comparative Analysis) 44
Figure 5-13: Net Thrust (Comparative Analysis) 45
Figure 5-14: Specific Thrust (Comparative Analysis) 46
Figure 5-15: SFC (Comparative Analysis) 47
Figure 5-16: Nozzle Exit Area (Comparative Analysis) 48

List of Tables

Table 4-1: Station Numberings 21

Table 4-2: Component Efficiencies and Losses 25

Table 5-1: Engine Operating Data at Design-Point (SLS) 33

Table 5-2: Net Thrust as %Gross Thrust at Off-Design Conditions 45

CHAPTER 1

Introduction

Nozzles used to propel fluids in engineering applications have been around since the 19th century. The commonly used nozzle configuration for supersonic flows involves a converging duct followed by a diverging duct. With the development of turbojet and turbofan engines during the World War II era, different nozzle configurations were experimented with, the ejector nozzle being one.[1] This chapter introduces the ejector nozzle and the motivation behind this research. A thermodynamic analysis of the ejector nozzle is discussed and the advantages and disadvantages are elucidated.

1.1 Motivation

Fixed-geometry nozzles used in propulsion applications can be operated for only a particular design condition. This causes a drastic decrease in performance at off-design conditions. In flight envelopes of military aircraft, there is a combination of multiple flight conditions for which the propulsion systems have to be operated. As a result, the fixed geometry, convergent-divergent duct nozzle is not often the best option due to its poor off-design performance. The ejector nozzle mitigates this by providing an “aerodynamic” variable geometry capability. The motivation behind this research is that a majority of prior research is based on experimental results. No unified analytical model exists that wholly encompasses the working of an ejector nozzle. In addition, many research codes developed by industry are proprietary and not available to academia for research.

The goal of this research study is to simulate an ejector nozzle-propulsion system and compare the on and off design performance with conventional nozzle propulsion systems.

1.2 Ejector Nozzle

1.2.1 Background

An ejector thrust augmentor is a device for increasing the thrust of a primary propulsive nozzle through fluid dynamic means. The maximum thrust of a propulsive nozzle is limited to a value which is far less than the potential thrust which would be available if a complete conversion from internal energy to kinetic energy could be achieved. This limit is essentially set by the ambient boundary conditions, specifically the ambient pressure into which the primary nozzle exhausts. The difference between the conversion of kinetic energy which occurs when a primary nozzle expands to a fixed exhaust plane pressure, and that which would occur if it expanded to match the local ambient pressure (the maximum potential thrust case), represents the source for ejector thrust augmentation.

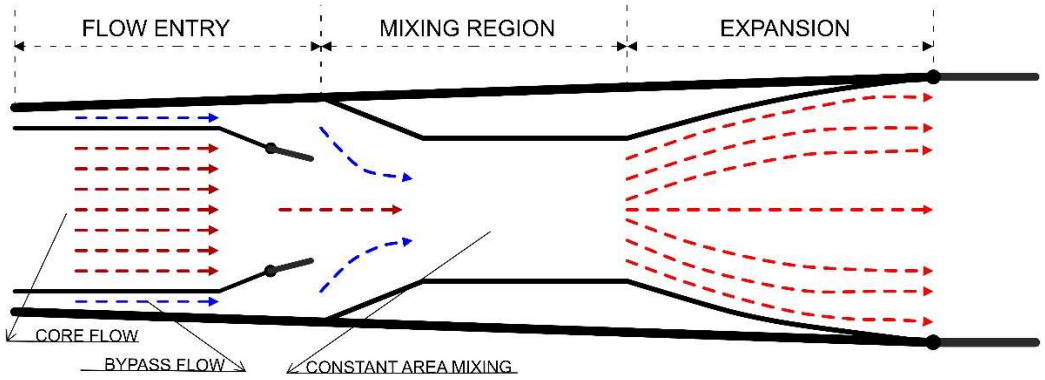

Figure 1-1: Ejector Nozzle Schematic

Figure 1-1 shows the schematic of the ejector nozzle. It utilizes the potential available in the primary nozzle fluid in the following way: The flow from the turbine exhaust (or afterburner, if present) is exhausted by a nozzle into a larger duct, usually called the ejector "shroud", where it interacts with, and induces motion in, the bypassed fluid in the shroud. The interaction between the two fluids for the steady flow situation is

primarily due to mixing and entrainment via the viscous shear layer formed between the two streams and results in an internal energy and momentum transfer from the primary flow to the secondary bypass flow. The mixed flow thus has a pressure and temperature condition intermediate between the initial conditions of the primary and secondary flow with a higher static pressure than the incoming flows. Also, due to the energy and momentum transfer, the kinetic energy of the mixed flow has increased, making the flow faster. This mixed flow, upon exhausting to the ambient back pressure, provides a greater total thrust due to the energy exchange which has taken place, than could have the primary nozzle alone. The ratio of this total mixed-flow thrust to the ideal thrust of a primary propulsive nozzle exhausting to the same ambient back pressure is called the thrust augmentation ratio ϕ.[2]

$$\phi = \frac{F_{ejector}}{F_{primary}} = \frac{Actual\ thrust\ produced\ by\ the\ ejector}{\begin{matrix} Thrust\ generated\ by\ the\ primary\ nozzle, \\ isentropically\ expanded\ to\ ambient\ pressure \end{matrix}}$$

$$= \frac{V_{ejector} \times \left(\dot{m}_p + \dot{m}_s\right)}{V_{primary} \times \dot{m}_p}$$

Now as the kinetic energy of the flow has increased at the mixer exit plane, this results in $V_{ejector} > V_{primary}$. By ensuring that $\dot{m}_s > 0$, the thrust augmentation factor, $\phi > 0$, confirming that the thrust provided by the ejector nozzle is higher than the thrust provided by the primary nozzle if the flow was expanded to the ambient back pressure.

1.2.2 Thermodynamic Analysis of the Ejector Nozzle

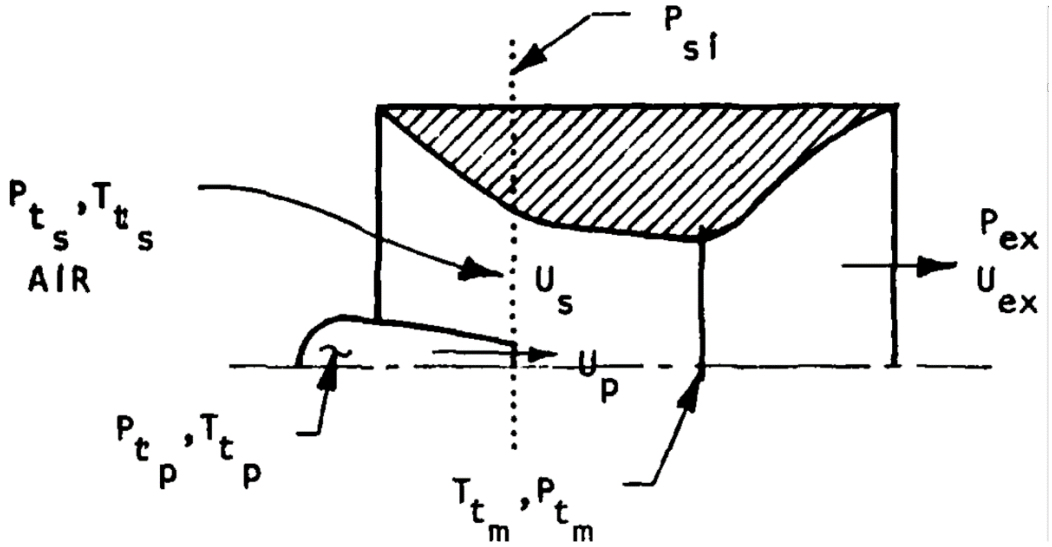

Figure 1-2: Ejector Nozzle Stations [2]

From Figure 1-2, P_t, T_t are the total pressure and total temperature of the flow. P_{si} is the static pressures at the inlet while T_{tm} and P_{tm} are the total temperatures and total pressures at the end of the mixing region. Subscripts *p*, *s* denote primary and secondary flow respectively. P_{ex} and U_{ex} denote the exhaust pressure and velocity respectively.

Primary core flow (from afterburner) is at a higher entropy level than the secondary bypass flow (from bypass duct). The primary nozzle is used to expand the core flow to ensure that the static pressures of the secondary and primary flow are equal ($P_{pi} = P_{si}$). The secondary flow gets entrained by the primary flow and they interact with each other by mixing. By the end of the mixing section, the flow is assumed to have completely mixed. The mixed flow total temperature is defined by the energy relationship,

$$T_{tm} = \frac{T_{tp} + \left(\dot{m}_s / \dot{m}_p\right) T_{ts}}{1 + \dot{m}_s / \dot{m}_p}$$

The mixed flow total pressure is a function of the thermodynamic process to achieve that temperature.[2] If the specific gas constant (R) of the flow is known, then the total density of the gas can be calculated from the ideal gas equation,

$$\rho_t = \frac{P_t}{RT_t}$$

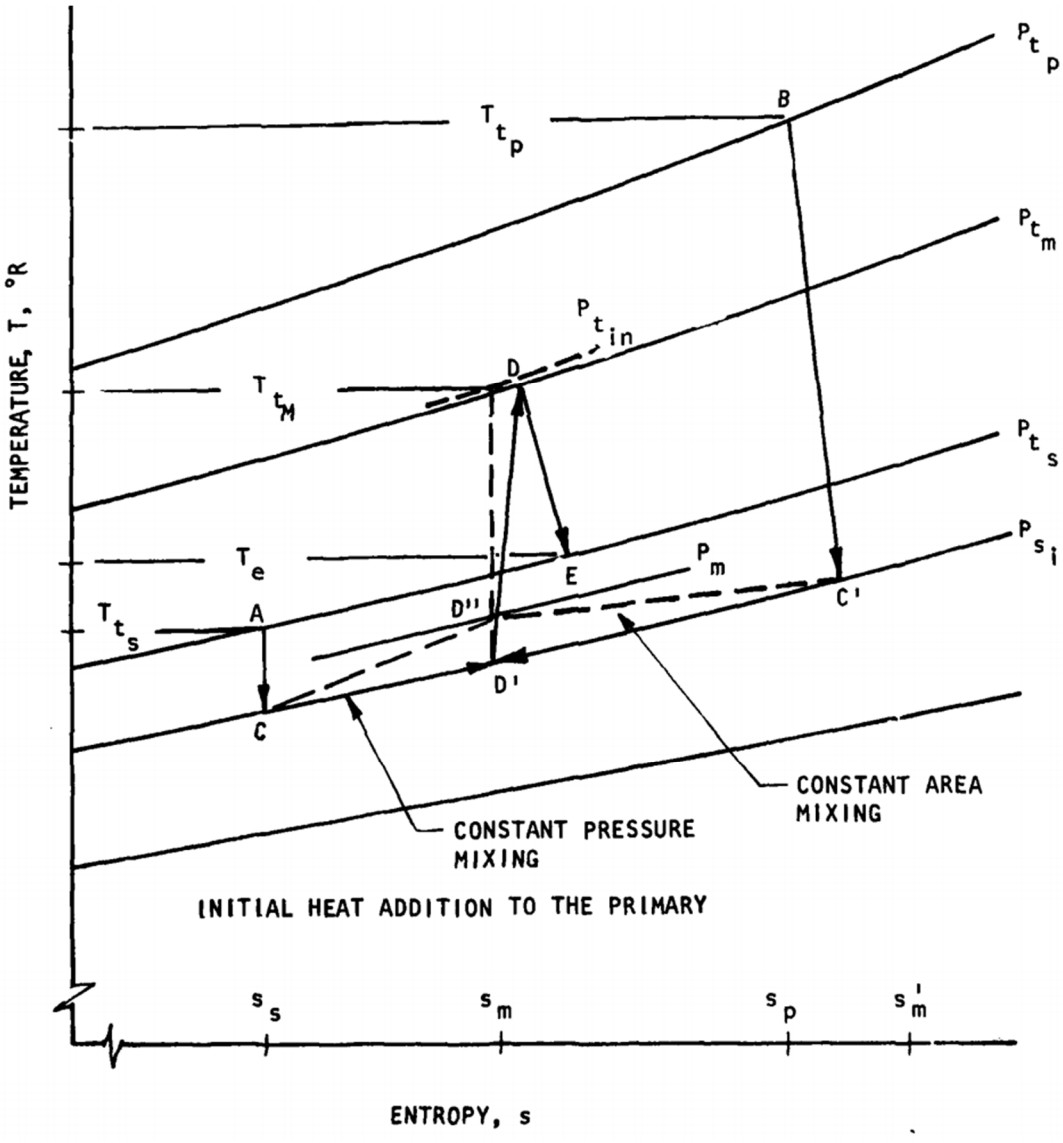

Figure 1-3: Temperature-Entropy Diagram for an Ejector Nozzle with Initial Heat Addition to the Primary Flow [2]

State Conditions:

A Initial State of Secondary Bypass Stream

B Initial State of Primary Core Stream

C Static State of Secondary Bypass Stream

C′ Static State of Primary Core Stream

D′ Initial Mixed State (constant pressure assumption)

D″ Initial Mixed State (constant area assumption)

D Completely Mixed State

E Exhaust State

Process A-C deals with the expansion of the secondary bypass flow in the duct to the ejector inlet. Expansion of the primary core flow takes place through Process B-C′. Modeling of mixing of the two fluid streams can be done based on two assumptions: constant area or constant pressure, which results in two separate curves. Processes C-D′:C′-D′ corresponds to constant pressure mixing while processes C-D″:C′-D″ corresponds to constant area mixing. Process D′-D (or D″-D depending on the mixing assumption) is when the two steams mix and attain uniform thermodynamic properties. The mixed flow then expands to the ambient pressure isentropically through Process D-E.

To define what happens inside the ejector, two approaches are considered: the physical phenomena approach and the control volume approach. The physical phenomena approach entails the application of finite element techniques in which mass, momentum and energy are conserved for discrete elements of the flow within the device to describe the interaction phenomena.[2] The control volume approach relies on application of the conservation of mass, momentum and energy to the bulk flow

properties between the upstream or interaction-entrance section and interaction exit zone, with little regard for what takes place physically in-between.[2]

Generally, the control volume approach provides a simple solution as it ignores complex boundary conditions, while the physical phenomena approach can give incorrect answers because of lack of knowledge on boundary conditions which have only minor bearing on the device performance.[2] In this thesis, a control volume analysis will be conducted. Discussions of this approach will be elaborated in the next chapter.

1.2.3 Advantages & Disadvantages of Ejector-Nozzle Turbofan Engines

Advantages:

- Off-design performance is improved in comparison with conventional propulsive systems.
- Exit static temperature is reduced which results in a stealthier engine.
- Thrust augmentation is provided.
- For a given thrust requirement, the nozzle exit area is smaller which leads to a smaller engine size.
- Secondary flow is also used to cool the engine.

Disadvantages:

- Expensive to develop as prototype testing is complicated.
- To ensure maximum ejector performance, complete mixing is required in the mixing chamber making the mixing chamber longer and hence increasing the length of the engine.

CHAPTER 2

Literature Survey

This chapter summarizes the references and their results that were used by the author in his research.

One of the earliest theoretical work on ejector augmentors was a paper published by von Karman in 1948.[3] This paper introduces the concept of the thrust augmentation factor, φ. He defines it as the ratio of the thrust produced by the ejector propulsive nozzle exhausting to the mixing plane static pressure to the ideal thrust of a primary propulsive nozzle exhausting to the same pressure. It also states that for an incompressible fluid, the maximum value of the augmentation is theoretically equal to 2 and is considerably lower for compressible fluids.

Kochendorfer [4] in his theory says that, "*for engines having low ejector pressure to ambient pressure ratios and a short cylindrical shroud, low or negligent mixing takes place*". This leads to the secondary fluid behaving as a moving solid boundary to the primary stream which enables it to expand to ambient pressure. The secondary stream reaches Mach unity speeds and hence chokes. This is called 'Fabri' choking.

Ejectors used as pumps and augmentors are widely described in a technical report by J. L. Porter and R. A. Squyers.[2] This report talks about the two different assumptions that can be made while constructing the mixer model: constant area mixer and constant pressure mixer. This report redefines the thrust augmentation ratio, φ as the ratio of the thrust produced by the ejector propulsive nozzle exhausting to the ambient pressure to the ideal thrust of a primary propulsive nozzle exhausting to the same back pressure. This is a more valid definition and leads to values of $\varphi \geq 2$. This report also provides equations that provide a closed-form analytical solution of the performance of the ejector nozzle.

Dutton and Carroll [6] say that "*the constant area mixer model has a broader range of possible solutions and is capable of predicting the aerodynamic choking phenomena called 'Fabri choking', whereas in the constant pressure mixer model, the wall contours necessary to produce constant pressure mixing are unknown*".

In Chow and Addy [7], nozzle pressure ratios are varied to obtain optimizing curves for the ejector. The paper also concludes that for supersonic primary and secondary streams, the flow is too fast for mixing to occur and that a moving inviscid slip line is formed acting as a solid boundary. This allows the primary flow to expand completely while the secondary flow is choked.

Fabri and Paulon [8] talk about the influence of mixing length on ejector performance. The performance of the ejector is not influenced by the length of the mixer as long as the latter is sufficient to make the establishment of the supersonic regime possible.

In a technical report for the US Army [9], the effect of partial mixing in the mixing chamber is discussed. Due to the insufficient length of the mixing chamber, incomplete mixing exists, thereby resulting in a non-uniform velocity profile at the exit of the mixing chamber. Thus, in order to predict reliably the effects of the incomplete (partial) mixing, an experimental investigation is necessary to obtain the pertinent data on pressure and velocity distributions at the exit of the mixing chamber. The equations developed are in terms of mixing length parameters that vary from case-to-case and have to be determined empirically. It also says that "*in selecting practical mixing chamber lengths, the considerations of the flow losses due to partial mixing may be of secondary importance".*

Johnson, Shumpert and Sutton [10] in their report for Lockheed-Martin say that the use of other than a constant area mixing section decreases ejector performance.

Heiser [11] says that thrust augmentation generally diminishes with forward speed, simply because it requires more energy from the primary flow to increase the kinetic energy of an already-moving secondary flow.

In a NASA research memorandum [1], it is found that having a fixed area exit nozzle compromises the performance at low Mach numbers where low overall pressure ratios exist. Losses in performance are due to the overexpansion of the nozzle. These losses can be eliminated by the use of a variable exit shroud. Test results show that this maximizes ejector performance.

Summarizing the information obtained, a control volume approach will be used. Due to the absence of experimental data on mixing chamber lengths for this study, a correction factor is assumed to account for incomplete mixing. At the end of the mixing plane, the mixed flow is exhausted to the atmosphere using a variable-exit area nozzle.

As a study on pressure ratios of ejector nozzle has already been performed [6,12,13], an optimization study of bypass ratios on performance of ejector nozzles is conducted.

CHAPTER 3

Numerical Propulsion System Simulation

This chapter begins by providing an overview of Numerical Propulsion System Simulation (NPSS). The individual components that make up the turbofan engine model are explained with the addition of the ejector nozzle setup.

3.1 Overview

The Numerical Propulsion System Simulation (NPSS) code was created through a joint effort by the gas turbine industry, NASA and universities to develop a state-of-the-art aircraft engine cycle analysis simulation tool. Written in the computer language C++, NPSS is an object-oriented framework allowing the gas turbine engine analyst considerable flexibility in cycle conceptual design and performance estimation. The object-oriented nature of NPSS enables nearly any conceivable engine architecture to be accurately modeled.[14] This feature will be explored by building the ejector setup in an existing configuration of a turbofan engine.[36]

3.2 Development of NPSS Code

The NPSS input text file has a structure resembling a computer program and its syntax conventions are closely aligned to the C++ language. In NPSS, engine components such as inlets, ducts, compressors, propellers, turbines, combustors, nozzles, shafts and mixers and their effects are represented as Element objects. These elements have the appropriate number of input and output ports attached to them and pass on values through predefined variables. Various engine components modeled as elements can be linked to each other through these ports and have individual linkages defined. These linkages are used to display outputs at each station.[36]

Several thermodynamic gas property packages are supplied with NPSS to support air breathing engine analysis (aircraft and industrial gas turbine engines). Their modular

design allows a user to select the desired package at run time. One package ("Janaf") offers flexibility and matches the NIST standard (NIST−JANAF, Revision 3) at the expense of some computational speed. A second package ("GasTbl"), created by Pratt & Whitney and based on NASA's "Therm," includes humidity calculations as well as some chemical equilibrium capabilities. The "CEA" thermodynamic package is an implementation of the NASA chemical equilibrium code. "allFuel," from General Electric, contains both gas properties and fuel properties. A fluid property table “FPT” package is also available. It allows users to define NPSS tables and/or functions to describe the thermodynamic properties of the fluid.[36]

Once the engine has been modeled, the design conditions must be set. It is a reference point from which each component is sized and engine performance is calculated for any predefined operating and flight conditions.

In engine design, there are six design parameters for gas turbine engines: maximum cycle pressure ratio (called overall pressure ratio or OPR), fan pressure ratio (FPR) for turbofan engines, turbine-inlet-temperature (TIT, T_{t4}), maximum cycle temperature (maximum afterburner exit temperature, T_{t7}), high-pressure compressor pressure ratio, and bypass-to-core mass flow ratio (called bypass ratio, BPR). These six parameters have the biggest effect on the engine performance figures of merit – specific thrust, specific fuel consumption. As inevitably happens, improvement in one engine figure of merit will come at a cost of at least one of the others, and it is rarely obvious that an improvement in say, fuel consumption, will offset an increase in engine size and weight.[14] For this reason cycle design parameters are varied over a range of values within material design limits to yield the optimum propulsion system from a set of many engine designs for a specific aircraft application.[14] To convert an ideal engine analysis to a real engine analysis, duct pressure losses, inlet recoveries, nozzle velocity coefficients,

compressor and turbine efficiencies, shaft mechanical efficiencies and mixer momentum losses must be set. Mattingly [15] lists approximate values for many of these inputs which can be used as estimates in the absence of detailed component designs.

The on-design case is executed followed by a set of off-design cases for each model run. In off-design runs, the engine which has been sized at design conditions, is made to run at any flight conditions for a particular flight speed, altitude, and throttle setting. For this reason off-design analysis is also called performance analysis. Hundreds of off-design cases are run to make certain the engine can operate over a flight envelope as well as to identify any unforeseen complications arising from potentially poor design choices[14]. In off-design test runs, each individual component that has been sized, has its design fixed. For compressors and turbines, maps are available that utilize scaling laws and matching to provide turbomachinery performance at off-design conditions. Nozzles may have variable area throat and exit properties.[36]

The solver is the part of NPSS that drives the model to a valid solution. The top-level assembly always contains a solver, which is created for the user. This solver receives a run command and is responsible for iteratively adjusting the values of the model independent variables in order to satisfy the dependent conditions in the system. If convergence cannot be achieved within a specified number of iterations, an error is returned for that case. For transient simulations, the solver also controls the progression of time within the run, providing a converged solution at each point in time.[36]

Many Elements contain predefined independents and/or dependents. Should the user choose the "default" solver setup, this information is automatically used to solve the cycle. User-defined independents and dependents may also be added to, or used instead of, the defaults provided. Further, constraints may be imposed on the solver's solution. Any assembly in an NPSS model may contain its own solver. When an assembly with a

solver is run, its solver attempts to converge that assembly by recursively calling any other assemblies it contains, and so on down to the bottom of the assembly tree. If an assembly does not have a solver, the independents and dependents in that assembly are handled by the solver in the assembly containing it. If an assembly has a solver, its independent variables are varied to satisfy its dependent conditions before control is returned to its parent assembly. A model may therefore contain a hierarchy of nested solvers, each responsible for solving a successively smaller portion of the model. The solver in the top level of the model is always responsible for controlling the time-step for transient simulations.[36]

Each assembly may define one "pre-solve" sequence of objects that is executed once before every converged point, an "inner-loop" solve sequence that is run during the solution process, and a "post-solve" sequence that is run after the point is converged. If an assembly does not have a solver, the pre-, inner-, and post-solve sequences are executed sequentially, once, and the flow of control is returned to the calling level.[36]

Therefore the basic steps in constructing and running a NPSS model are: [36]

1. Specify a thermodynamics package.
2. Instantiate the necessary Elements, Subelements, Ports, and Assemblies. Also create any necessary functions and table. This step may involve using preprocessor commands to include pre-written components distributed with NPSS, or user written components. It may also involve use of Creation Method Facilities.
3. Link the model's ports.
4. Insure that the model's execution sequence is satisfactory, and add any necessary items to the preExecutionSequence or postExecutionSequence attributes of each assembly’s Executive.

5. Define input and output as required.
6. Set up the model's solver or solvers.
7. Define the desired cases, and run the model, modifying the solver setup as required.

The equations of each component used in the modeling of a turbofan engine can be found in Mattingly.[16] Maps are used for turbomachinery while a simple inlet model is inbuilt in NPSS. The equations used for modeling the mixer element are discussed.

The mixer conserves energy, continuity, and momentum when mixing two streams into one. At design point the user needs to provide a Mach number for the primary entrance flow which determines the primary entrance area. The secondary entrance area is determined by varying the Mach number until the static pressure of the two streams is equal. The exit area is determined by adding the two entrance areas together (constant area mixer). The incoming impulse term is calculated from,

$$Impulse\ (mixed) = \left(P_{s1} \times A_1 + \frac{\dot{W}_1 \times V_1}{g}\right) + \left(P_{s2} \times A_2 + \frac{\dot{W}_2 \times V_2}{g}\right)$$

Where,

P_S — static pressure

V — velocity

A — physical area

g — acceleration due to gravity at sea level

$\dot{W}$ — weight flow rate

$_{1,2}$ — denotes primary or secondary flow

The outgoing impulse term is calculated from,

$$Impulse\ (output) = \left(P_s \times A + \frac{\dot{W} \times V}{g}\right)$$

By iterating the pressure term based on the impulse error between the mixed and output values, the final impulse value is calculated which leads to a flow that is balanced in continuity, momentum and energy.

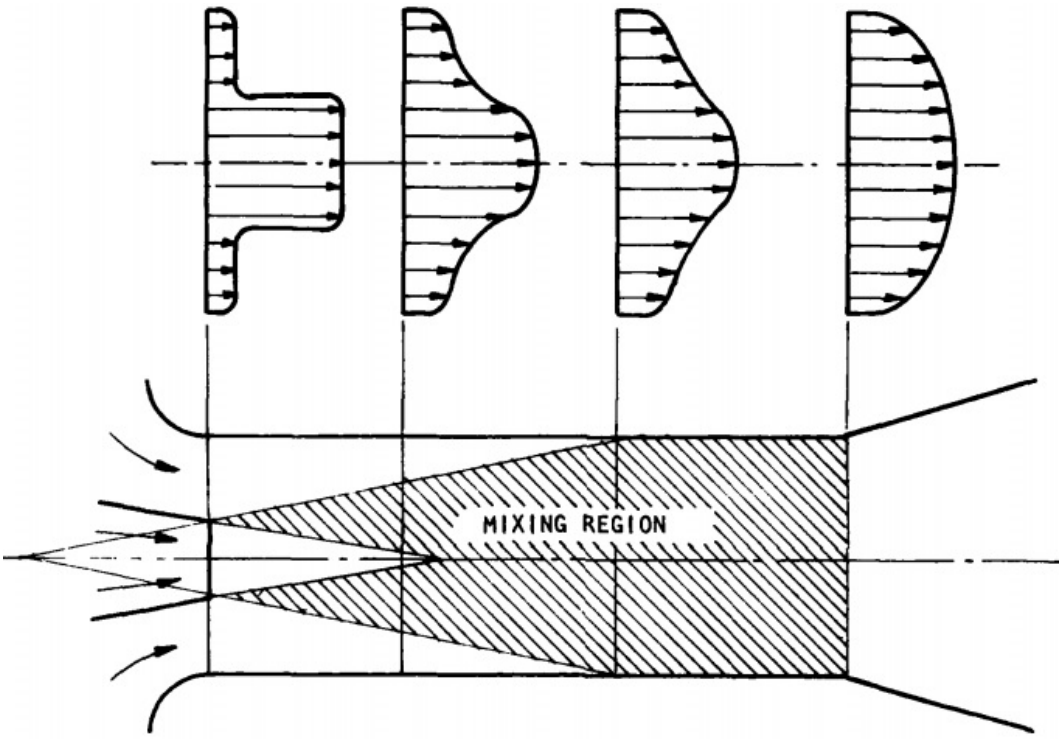

Figure 3-1: Typical Velocity Distributions in an Ejector Mixing Chamber [2]

The combination and sequence of elements that are modeled, define the configuration of the engine.

CHAPTER 4

Simulation Setup

This chapter describes the NPSS model of the ejector nozzle-based low bypass ratio turbofan engine and gives the on-design and off-design conditions.

4.1 Model Flowchart

The basic Brayton cycle gas turbine engine has three vital components: compressor, burner and turbine. For propulsive applications involving turbofan engines, an inlet, nozzle, bypass duct with a splitter and mixer is also added. Figure 4-1 gives the ejector-nozzle turbofan engine diagram and Figure 4-2 gives a detailed schematic of how the engine configuration is modeled in NPSS.

It starts with the declaration of the ambient element. That is followed by the inlet element and the fan element. The fan element uses a low pressure compressor map that is built into NPSS. Following the fan, a splitter plate element is used to bypass a part of the core flow into duct elements. This splitter is governed by the fan bypass ratio (FBP). The core flow is then compressed by a high pressure compressor element before injecting it into the combustion chamber element.

Methane with a LHV of 21500 Btu/lbm is used as fuel for its superior heat of combustion.[18] To prevent thermal stresses on turbine blades, a temperature constraint of 3600 R is placed on the turbine inlet temperature (or T_{t4}), a bottleneck on aircraft engine performance. The core flow expands through the high pressure turbine (HPT) element first before expanding in the low pressure turbine (LPT) element. A high speed shaft element is used to couple the HPT and HPC while a low speed shaft element is used to couple the LPT and fan.

The bypass air passes through a splitter element which is governed by the ejector bypass ratio (EBP). A part of the bypass air is then mixed with the core flow in a mixer

element which burns in the afterburner. Another temperature constraint of 4000 R is put on the nozzle inlet temperature (T_{t7}) to ensure that the nozzle shroud does not mechanically fail. A bleed element is used to collect the ejector bypass duct flow or the secondary flow. The thermodynamic properties of this flow will be utilized in the ejector nozzle equations.

The ejector nozzle setup begins with the primary convergent-divergent nozzle element expanding the core flow to the ambient pressure. The thermodynamic properties of the flow are used in the following equations to simulate the ejector nozzle.

The total temperatures of the primary and secondary flow, T_{tp} and T_{ts} and the bypass ratios, FBP and EBP are used to attain the total temperature of the mixed flow, T_{tm}.

$$T_{tm} = \frac{T_{tp} + \beta T_{ts}}{1 + \beta}$$

where β = FBP x EBP = the fraction of air flow rate going into the ejector nozzle mixing section

The mixed flow total temperature is then used to calculate the exit velocity of the thrust augmenting mixed flow, u_{ex},

$$u_{ex} = \sqrt{\frac{2\gamma R}{\gamma - 1}(T_{tm} - T_{ex})}$$

where,

$$T_{ts} < T_{ex} < T_{ex(primary)}$$

By introducing a factor for T_{ex}, which will be denoted by ‘α’, the extent of mixing of the primary flow and secondary flow, in effect, the energy and momentum transfer between the two flows can be controlled.

As T_{ex} is a function of the kinetic energy of the mixed flow, $\alpha * T_{ex}$ can be used to study the effect of extent of mixing of the flows, with $\alpha = 0$ for 100% mixing (the exit static temperature has reached the total temperature of the secondary stream, resulting in maximum increase of kinetic energy) and $\alpha = 1$ for 0% mixing (the exit static temperature is the same as the exit static temperature of the primary nozzle resulting in no change of kinetic energy).

Once the exit velocity of mixed flow is known, it is used in the thrust equation to obtain the augmented thrust of the ejector nozzle.

$$F_{ejector} = \dot{m} \times u_{ex}$$

Using NPSS to calculate the thrust of the primary nozzle expanding to the ambient back pressure, the thrust augmentation ratio of the ejector nozzle can be obtained.

$$\phi = \frac{F_{ejector}}{F_{primary}} = \frac{Actual\ thrust\ produced\ by\ the\ ejector}{Thrust\ generated\ by\ the\ primary\ nozzle,\ isentropically\ expanded\ to\ ambient\ pressure}$$

Studies have shown that ejector thrust augmentors for aerospace applications generally have a thrust augmentation ratio of $\phi < 1.4$. Hence in this thesis, an alpha value is appropriately chosen that gives $\phi = 1.15$.

From Figure 4-1, it is found that $\alpha = 0.8$ best fits this condition and provides realistic engine performance values.

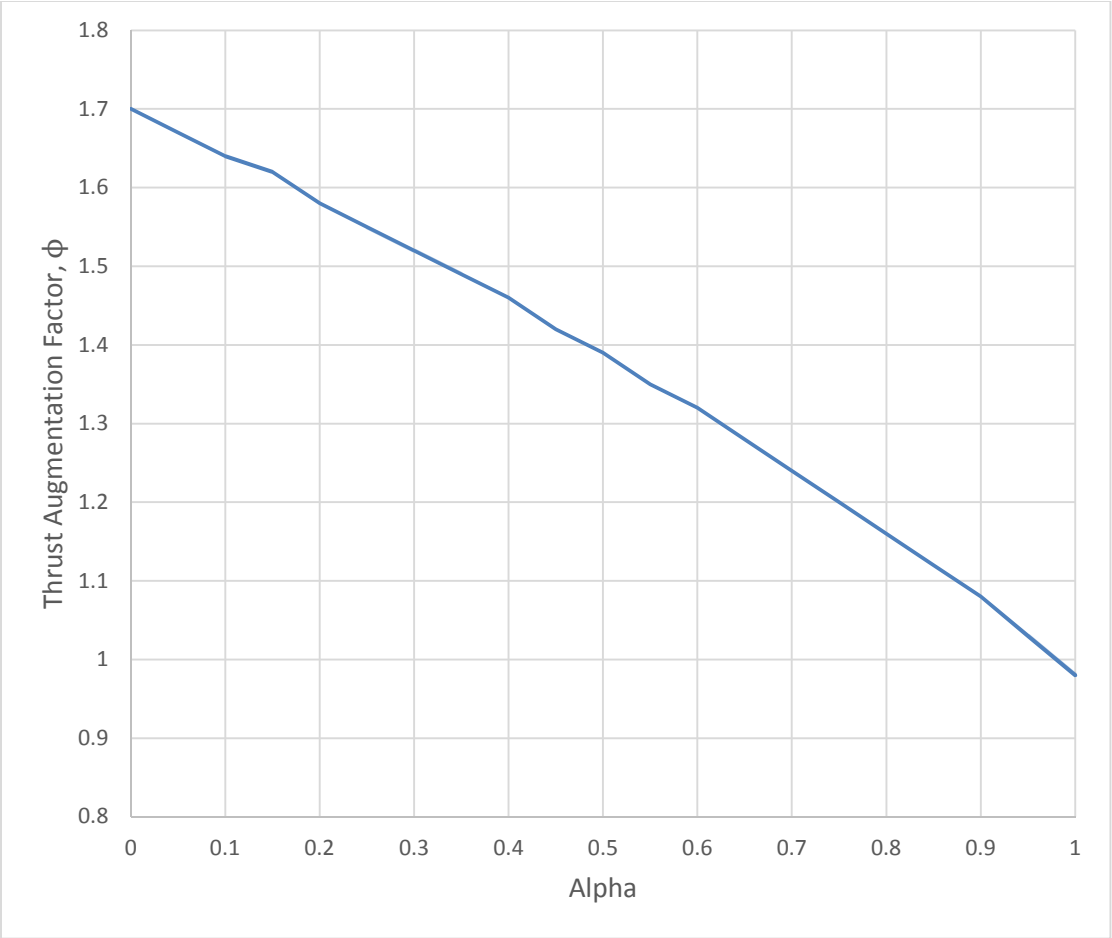

Figure 4-1: Effect of Alpha on Thrust Augmentation Ratio

The station numbering and their SAE counterpart are given below:

Table 4-1: Station Numbering

Station Exit	NPSS Station numbers	SAE Nomenclature
Ambient	000	0
Inlet	020	2
Fan	025	2.5
Fan Bypass Splitter	130	13
Bypass Duct	145	16
HP Compressor	030	3
Combustion Chamber	040	4
High Pressure Turbine	045	4.5
Low Pressure Turbine	050	5
Ejector Bypass Splitter	245	—
Bypass Duct	275	—
Mixer	060	6
Afterburner	070	7
Primary Nozzle	090	9

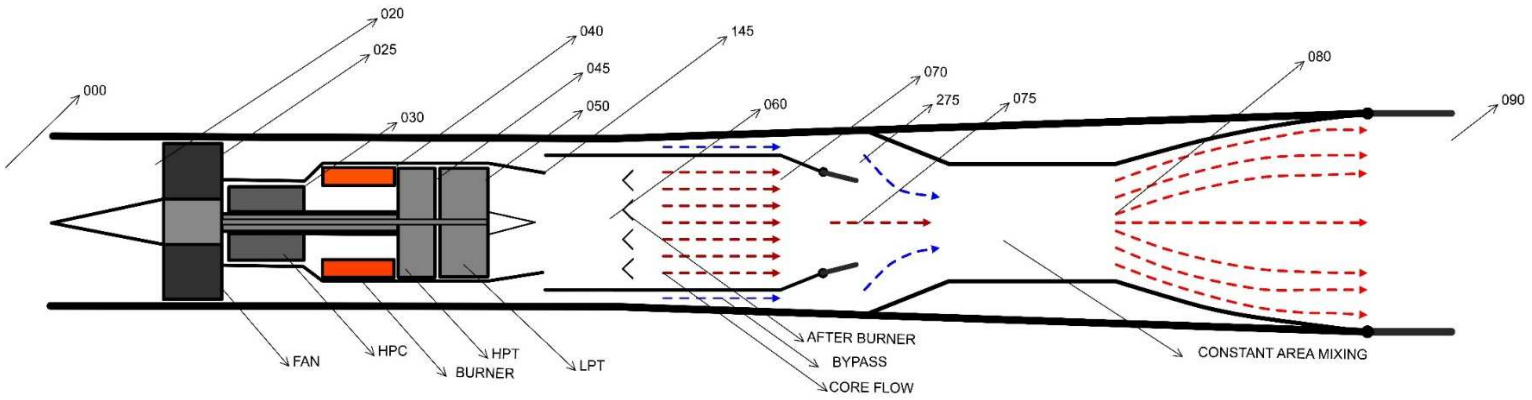

Figure 4-2: Ejector-nozzle Turbofan Engine Diagram with station numbering

(Not to scale)

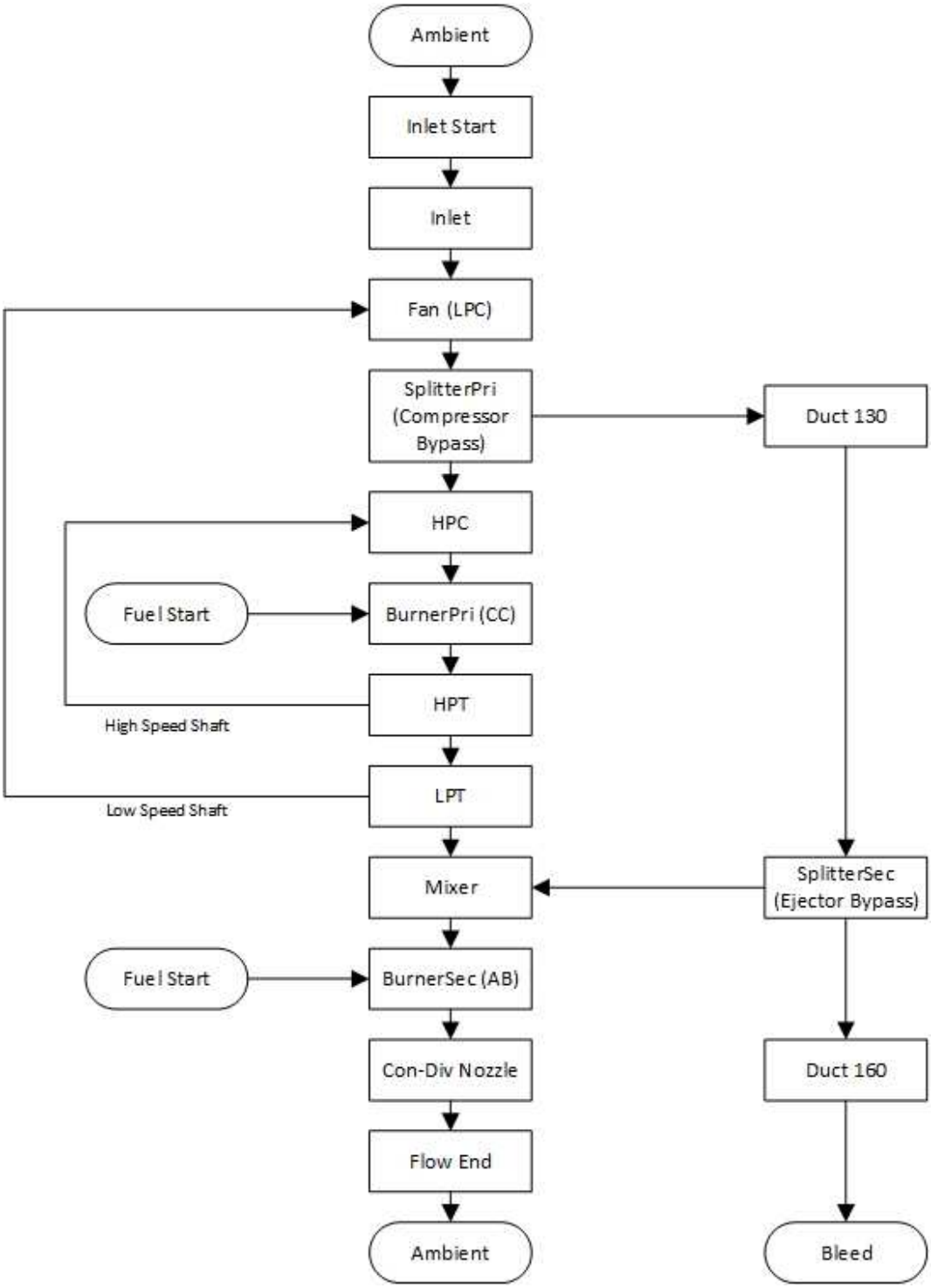

Figure 4-3: Ejector-based Turbofan Engine NPSS Element Flowchart

4.2 On-Design

On-design conditions are used to size the engine for a given thrust requirement with constraints on the turbine inlet and nozzle inlet temperatures. Data required by NPSS includes the ambient conditions, compressor pressure ratios, efficiencies (for non-ideal engine analysis) and individual component losses. These values are taken from Mattingly's [15] component performance – level 4 technology.

A majority of published engine data for military engines is based on sea-level-static (SLS) conditions. This is because most experimentation of engines is conducted at sea level static conditions and also because the aircraft is the sized to meet takeoff thrust requirements. Hence SLS is chosen as the on-design condition for this research. As a result an ambient Mach number of 0 and altitude of 0 feet is set. The maximum inlet pressure recovery was set at 0.96.[15]

From the database in Kerrebrock [19], modern military engines typically have an overall compressor ratio maximum of 36 with the fan providing a pressure ratio of 5. As the engine discussed in this thesis replicates that, the same pressure ratios are selected. Hence $\pi_c = 36$, $\pi_f = 5$ and $\pi_{hc} = 7.2$ are set as on-design reference conditions. NPSS has two inbuilt compressor files that are used for matching: the low pressure compressor file is linked to the fan compressor while the high pressure compressor map is linked to the high pressure compressor. NPSS inputs efficiencies in terms of the adiabatic efficiencies, η_c while the polytropic efficiency, e_c, is provided in Mattingly's text.[15] The polytropic efficiencies of the low pressure compressor (or fan), high pressure compressor, high pressure turbine and low pressure turbine are 0.89, 0.90, 0.89 and 0.89 respectively. The values of e_c are converted to η_c by the following formula:

$$\eta_c = \frac{\pi_c^{\frac{(\gamma-1)}{\gamma}} - 1}{\pi_c^{\frac{(\gamma-1)}{\gamma e_c}} - 1}$$

A total pressure ratio loss of 0.05 and combustion efficiency of 0.99 for the combustion chamber element and afterburner element are set. Total pressure ratio loss of 0.05 is set for the duct elements and nozzle elements. The primary nozzle element expands the core flow to the ambient pressure. The equation model discussed in the previous section, calculates the ejector nozzle performance. These values are then fed back into NPSS for iteration and the process is repeated until the solution converges with the ejector nozzle fulfilling the thrust requirement imposed by the user.

The maximum possible turbine inlet temperature is set at T_{t4} = 3600 R and the nozzle inlet temperature at T_{t7} = 4000 R.

The efficiency and pressure losses of individual components of the engine are set. The values are summarized in Table 4-2.

Table 4-2: Component Efficiencies and Losses [15]

Diffuser (Pressure Ratio Loss)	π_{dmax}	0.96
Fan Compressor (Adiabatic Efficiency)	η_{fc}	0.86
High Pressure Compressor (Adiabatic Efficiency)	η_{hc}	0.8
Burner (Adiabatic Efficiency and Pressure Ratio Loss)	η_b	0.99
	π_b	0.95
High Pressure Turbine (Adiabatic Efficiency)	η_{hpt}	0.90
Low Pressure Turbine (Adiabatic Efficiency)	η_{lpt}	0.90
Nozzle (Pressure Ratio Loss)	π_n	0.97
Ducts (Pressure Ratio Loss)	π_d	0.95

4.3 Off-Design

In off-design, NPSS fixes the base design of each component and runs the trials. For the off-design performance analysis, three operating conditions are defined for a certain part of flight envelope that a military aircraft will encounter on its mission. They are:

1. Supersonic Cruise (Or Supercruise)
2. Dash
3. Subsonic Cruise

Supercruise conditions take place at an altitude of 15 km with a flight Mach number of 1.6. The afterburner is switched off.

Dash conditions take place at an altitude of 15 km with a flight Mach number of 2.0. The afterburner is switched on.

Subsonic Cruise conditions take place at an altitude of 12 km with a flight Mach number of 0.85. The afterburner is switched off.

4.4 Comparative Models Setup

Once the ejector-based engine has been optimized for design and off-design conditions, it is compared with three different engine configurations, which are modeled with the same operating parameters. They are:

1. Unmixed Flow Low BP Turbofan Engine
2. Mixed Flow Low BP Turbofan Engine
3. Turbojet

The engine diagram and model flowcharts for each configuration that show its working, are given below.

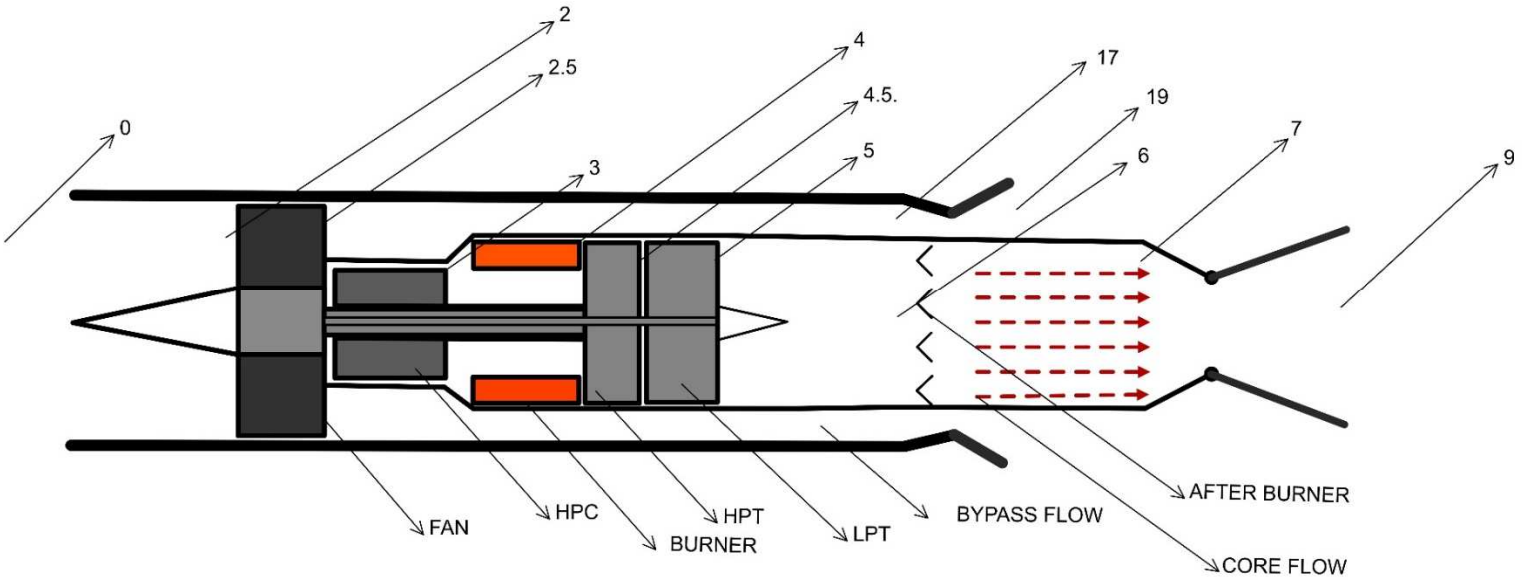

Figure 4-4: Unmixed flow Turbofan Engine Diagram

From Figure 4-4, the unmixed flow turbofan engine has two nozzles, the primary and secondary nozzle. Core flow expands to the ambient condition through the primary nozzle and the secondary flow expands through the secondary nozzle. Both the core and bypass flows do not interact until they are outside the engine.

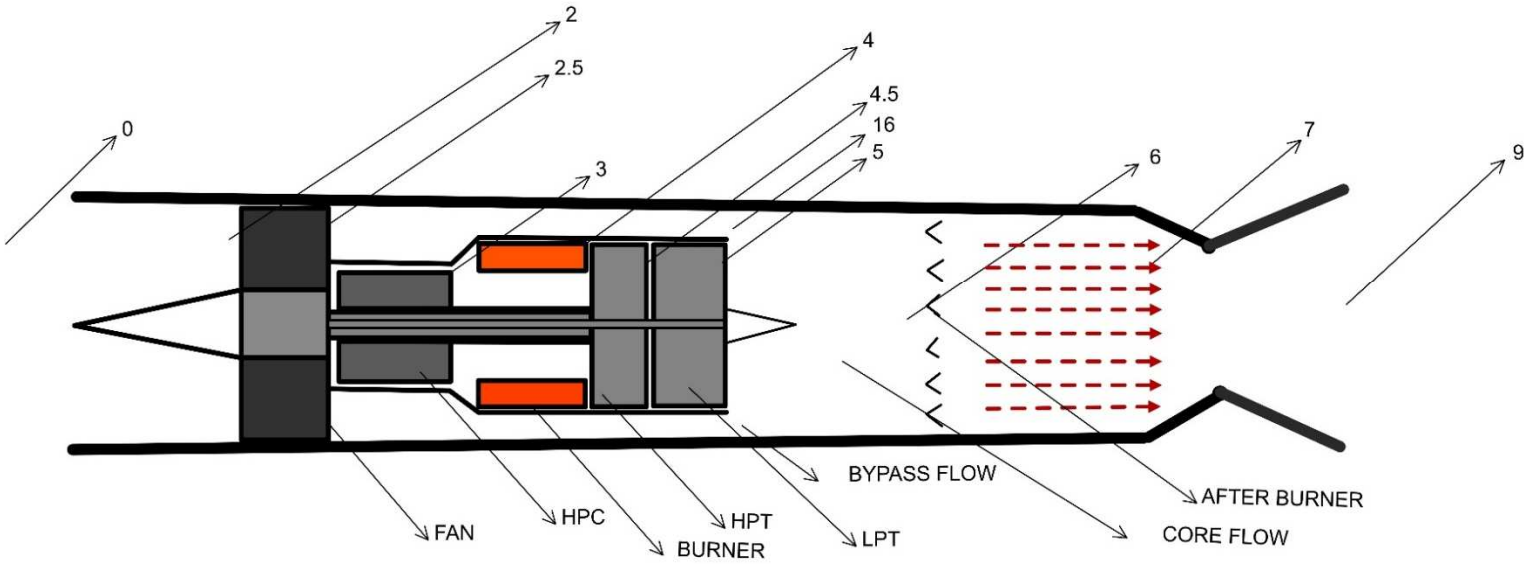

Figure 4-5: Mixed flow Turbofan Engine Diagram

Figure 4-5 shows the mixed flow turbofan engine. In this engine configuration, all the bypassed air gets mixed with the core flow upstream of the afterburner and the mixed flow is expanded through the nozzle to the ambient conditions.

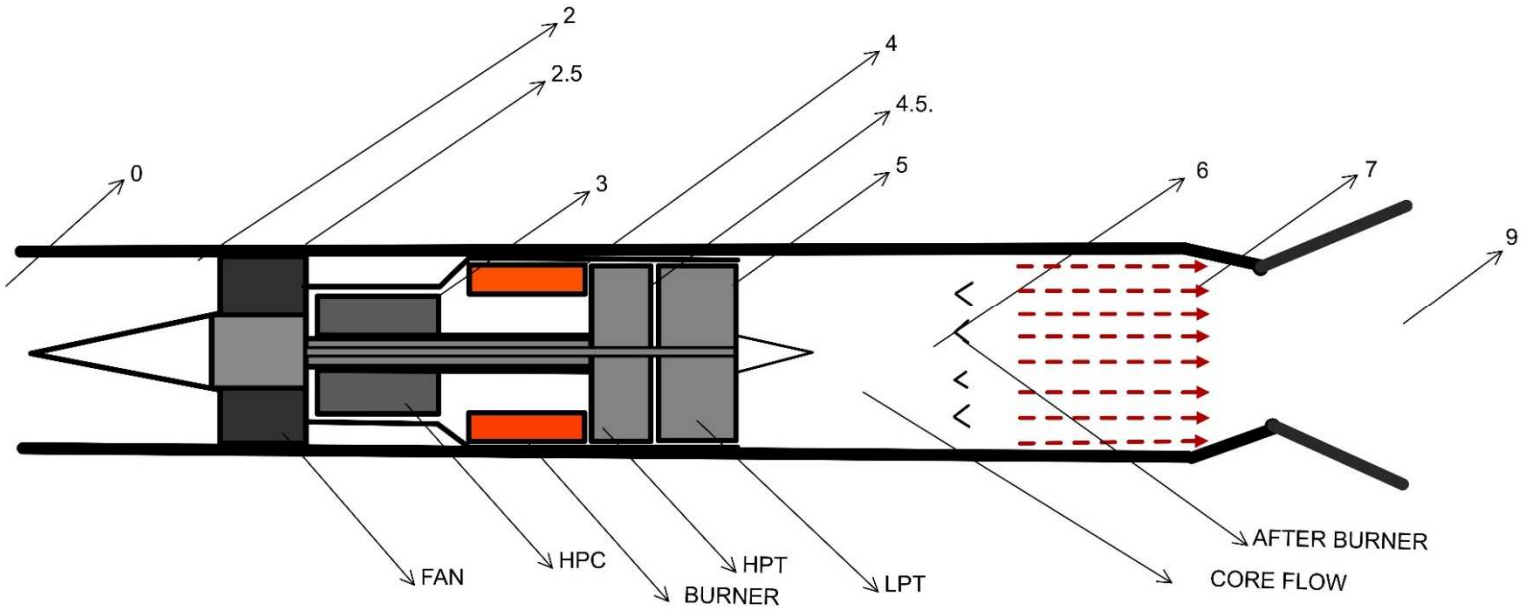

Figure 4-6: Turbojet Engine Diagram

Figure 4-6 shows the Turbojet engine. All the engine's mass flow goes through the core and there is no bypass. The core flow is then expanded to the ambient by a converging-diverging nozzle.

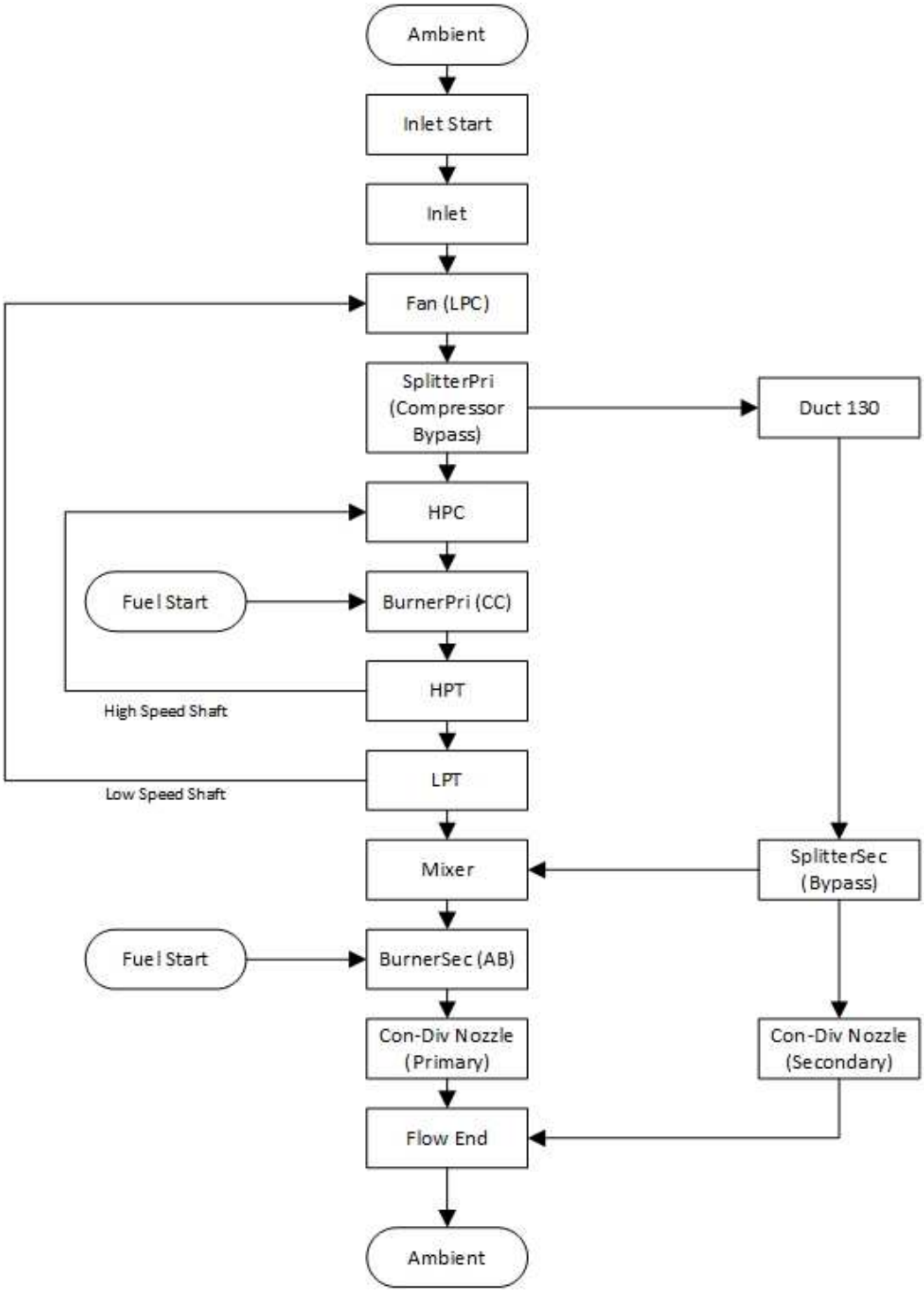

Figure 4-7: Unmixed Flow Low BP Turbofan Engine NPSS Flowchart

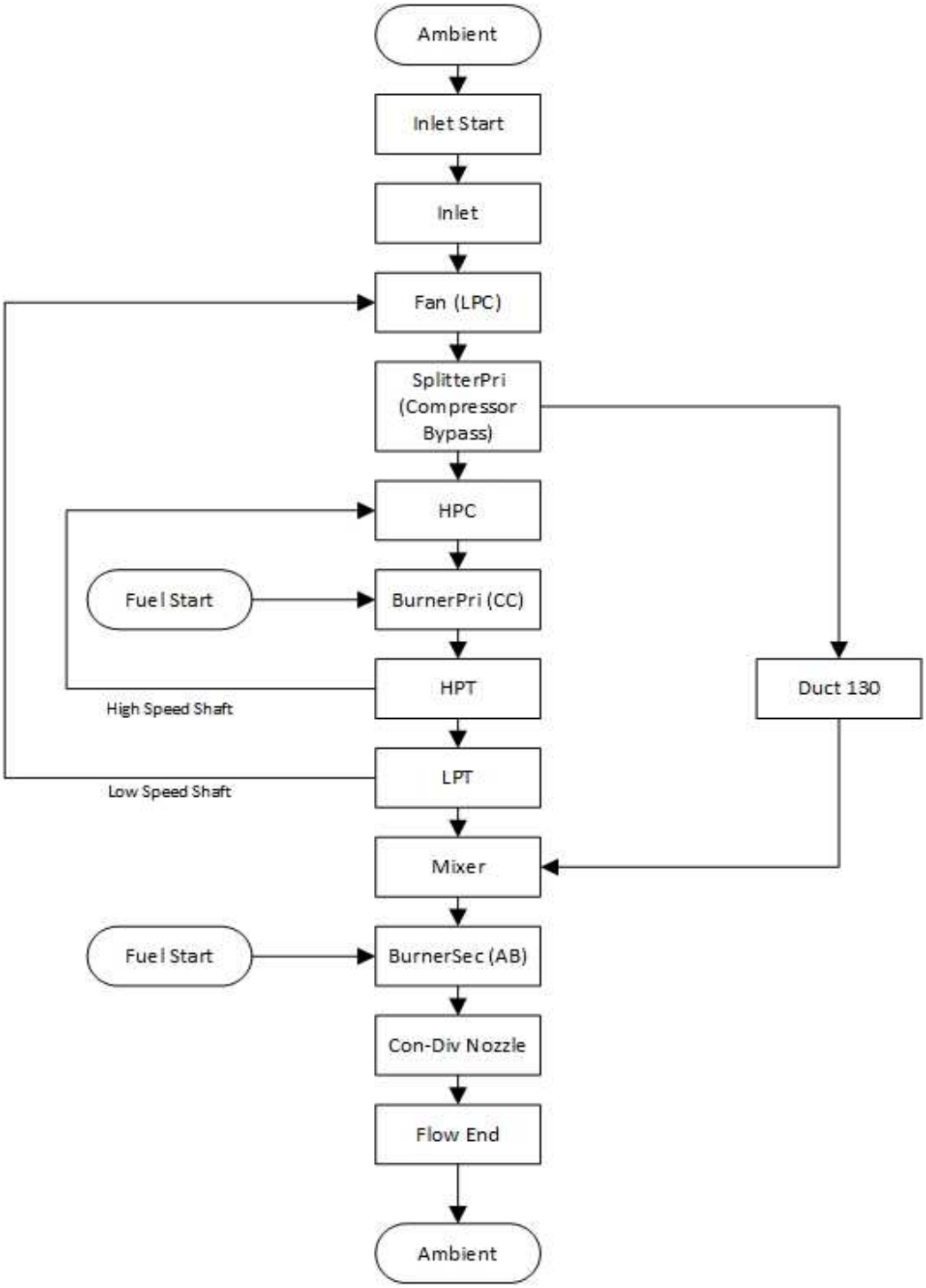

Figure 4-8: Mixed Flow Low BP Turbofan Engine NPSS Flowchart

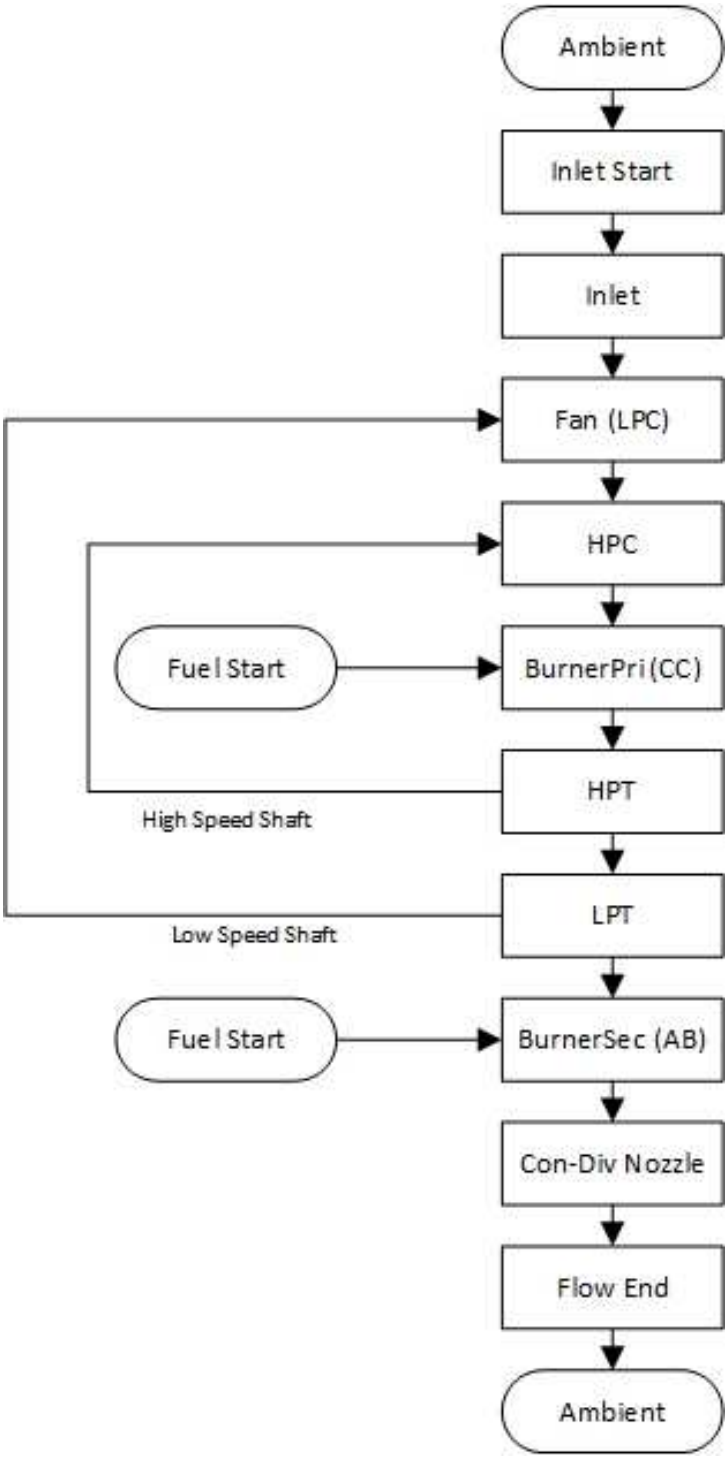

Figure 4-9: Turbojet Engine NPSS Flowchart

CHAPTER 5

Results

The trial runs for on-design and off-design analysis are conducted and the results are summarized in this chapter. Section 5.1 deals with optimization of the bypass ratios (fan and ejector) based on selected performance parameters. Section 5.2 contains the results from the comparative analysis performed between the optimized ejector-based turbofan and three different engine configurations.

5.1 Engine Optimization

All data presented in this section is for the on-design condition (sea-level static). Fan bypass ratio is varied from 0.1 to 0.9. Each dot in the following graphs denotes an individual engine that has been sized with the particular bypass ratios for a thrust requirement of 30000 lbf. FBP is the fan bypass ratio and EBP is the ejector bypass ratio. The fan bypass is the fraction of the core flow that gets diverted into the secondary ducts. The ejector bypass is the fraction of the fan bypass air that gets into the ejector mixer while the rest of fan bypass flow gets mixed with the core flow out of the turbine exhaust. Ejector bypass ratio is varied from 0.1 to 1.0.

Table 5-1: Engine Operating Data at Design-Point (SLS)

Altitude	0 ft
Flight Mach Number	0
Required Trust	30000 lbf
Turbine Inlet Temperature	3600 R
Primary Nozzle Inlet Temperature	4000 R
Overall Compressor Pressure Ratio	36
Fan Pressure Ratio	5
HP Compressor Ratio	7.2

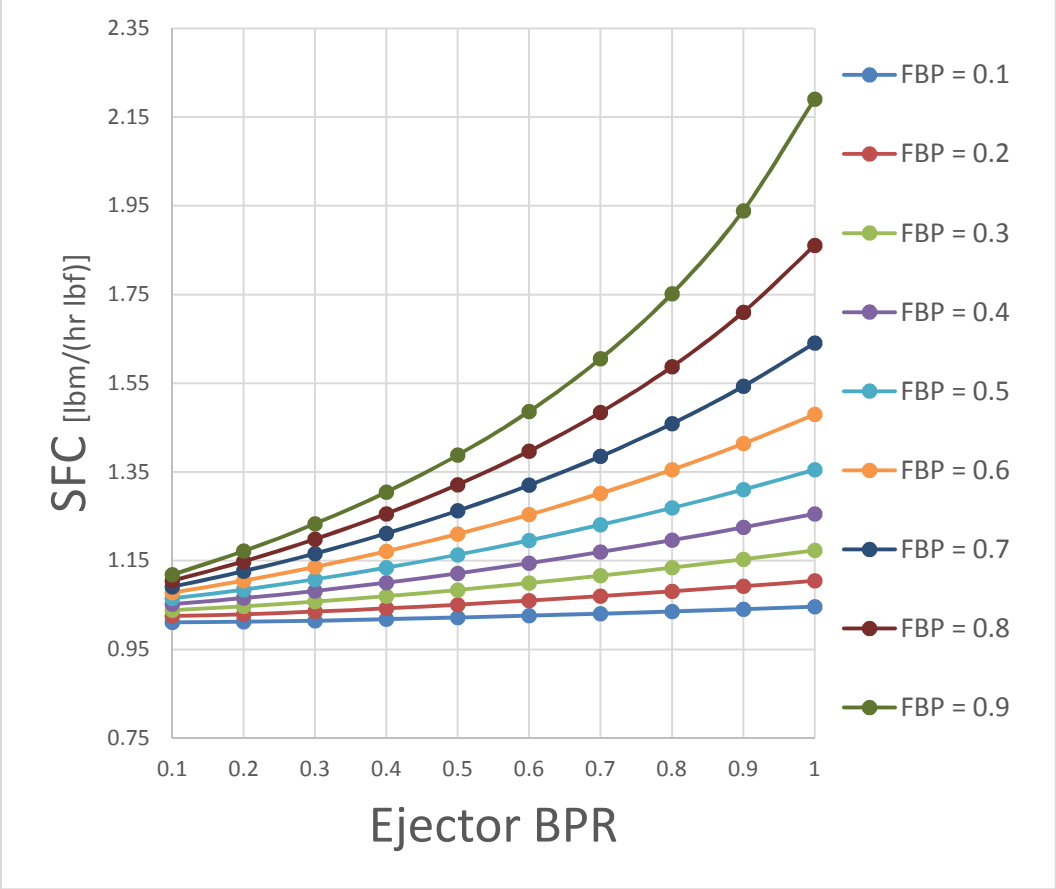

Figure 5-1: Variation of SFC as a function of Ejector Bypass Ratio at different Fan Bypass Ratios

Intuitively, we know that a higher fan bypass ratio would lead to lower fuel consumption and hence SFC as more air is bypassed from the burners. But from Figure 5-1, we find the opposite is true with the lowest fan bypass ratio providing the lowest SFC. This is caused by the thrust requirement that is defined for engine sizing leading to the engine having to burn enough fuel to make sure the requirement of a thrust output of constant 30000 lbf has met. Also we find that the lowest EBP for a given FBP has the lowest SFC due to the afterburner having to burn less fuel.

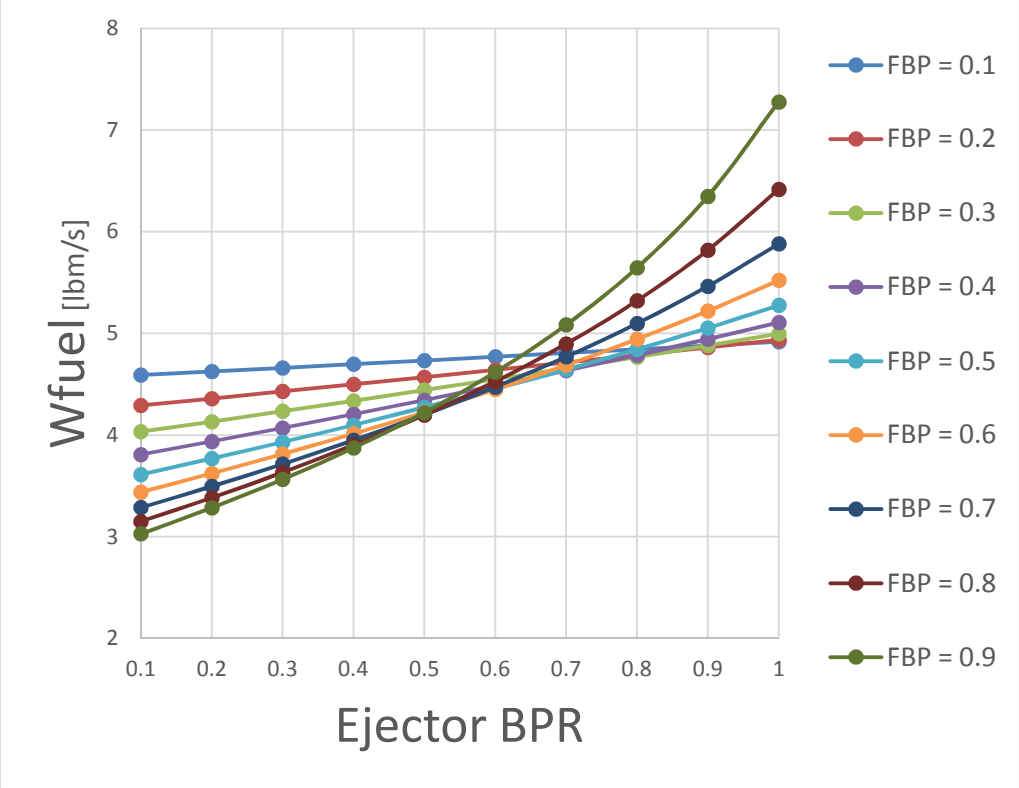

Figure 5-2: Variation of Combustion Chamber Fuel Flow Rate as a function of Ejector Bypass Ratio at different Fan Bypass Ratios

From Figure 5-2, we see that the highest combustion chamber fuel flow rate is for FBP = 0.1, while FBP = 0.9 has the lowest fuel consumption at low EBP. But as the EBP increases, the trend reverses with FBP = 0.9 having the highest fuel consumption. This reversal of trend occurs between EBP = 0.5 to 0.8.

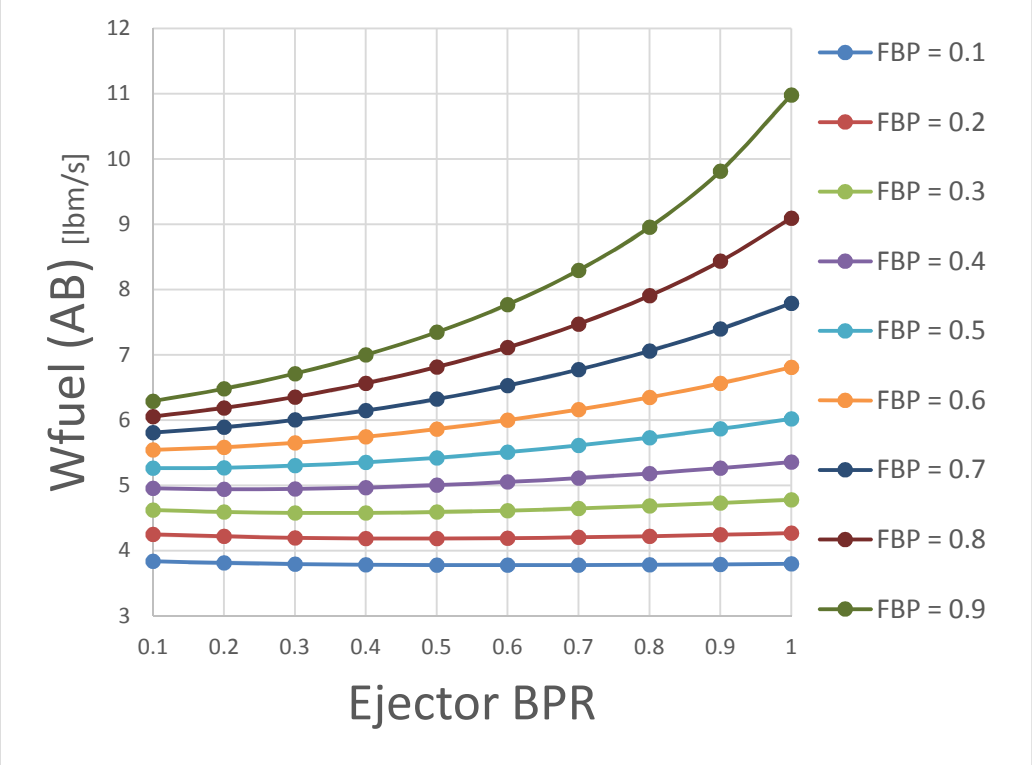

Figure 5-3: Variation of Afterburner Fuel Flow Rate as a function of Ejector Bypass Ratio at different Fan Bypass Ratios

Figure 5-3 shows that as the FBP increases, the afterburner has to burn much more fuel to reach the thrust requirement, due to the temperature constraint at the nozzle inlet of 4000 R. The core flow for lower FBPs already has a high total temperature, thus the afterburner burns minimum fuel.

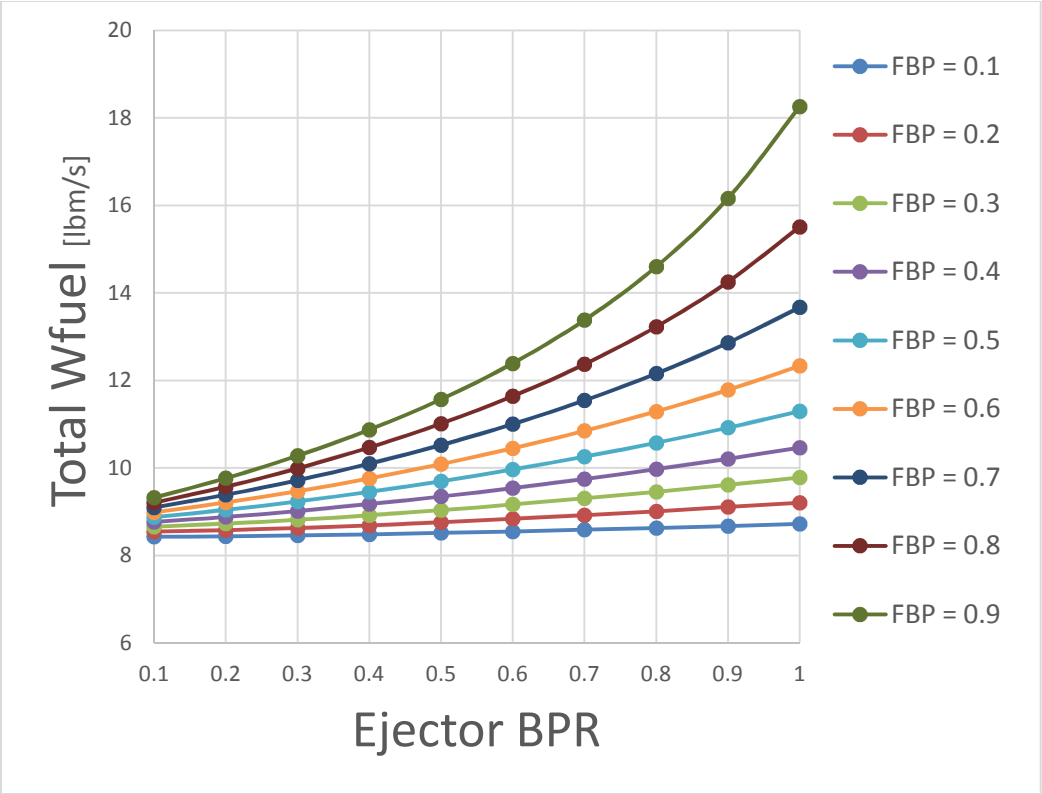

Figure 5-4: Variation of Total Fuel Flow Rate as a function of Ejector Bypass Ratio at different Fan Bypass Ratios

As a result, total fuel burnt increases as FBP increases (Figure 5-4), leading to a higher SFC at higher FBP. Also, the ejector splitter bypasses part of the air from the afterburner and mixes it in the ejector nozzle. Hence lower EBPs lead to lower SFC. The effect is magnified at higher FBPs as the magnitude of air in the bypass ducts increase exponentially (at FBP=0.1, the percentage of total mass flow at EBP = 0.1 and 0.9 is only 1 percent and 9 percent; at FBP=0.9, the percentage of total mass flow at EBP = 0.1 and 0.9 is 9 percent and 81 percent).

Specific thrust is defined as the ratio of net thrust to the air mass flow rate. It is a measure of the bulkiness of an engine and gives an idea of the mass and volume occupied by the engine.[21] In these trials, the net thrust is kept constant for all cases at

30000 lbf, and the mass flow rate is varied while sizing the engine resulting in an easier method of comparison since higher mass flow rates tend to make the inlet bigger by lowering the specific thrust thereby making the engine bulkier. Low specific thrust engines are larger and quieter and are used majorly for civil aviation where the engine is located under the wing. High specific thrust engines are much smaller but very loud. They are used mostly in military aircrafts where the engine is located inside the airframe.[22]

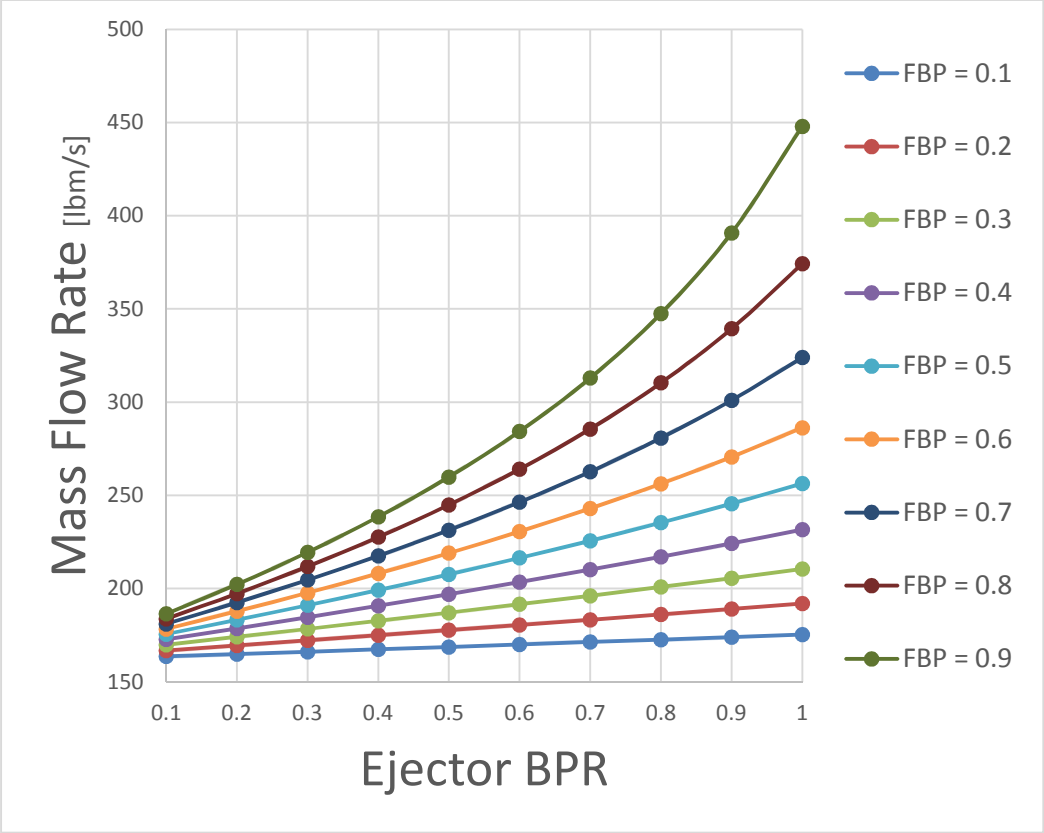

Figure 5-5: Variation of Mass Flow Rate as a function of Ejector Bypass Ratio at different Fan Bypass Ratios

Figure 5-5 shows that at low FBPs and EBPs, mass flow rates are minimum leading to an increase in specific thrust resulting in a smaller, less bulky engine. Figure 5-6 reinforces this result with specific thrust decreasing as the FBP and EBP increases.

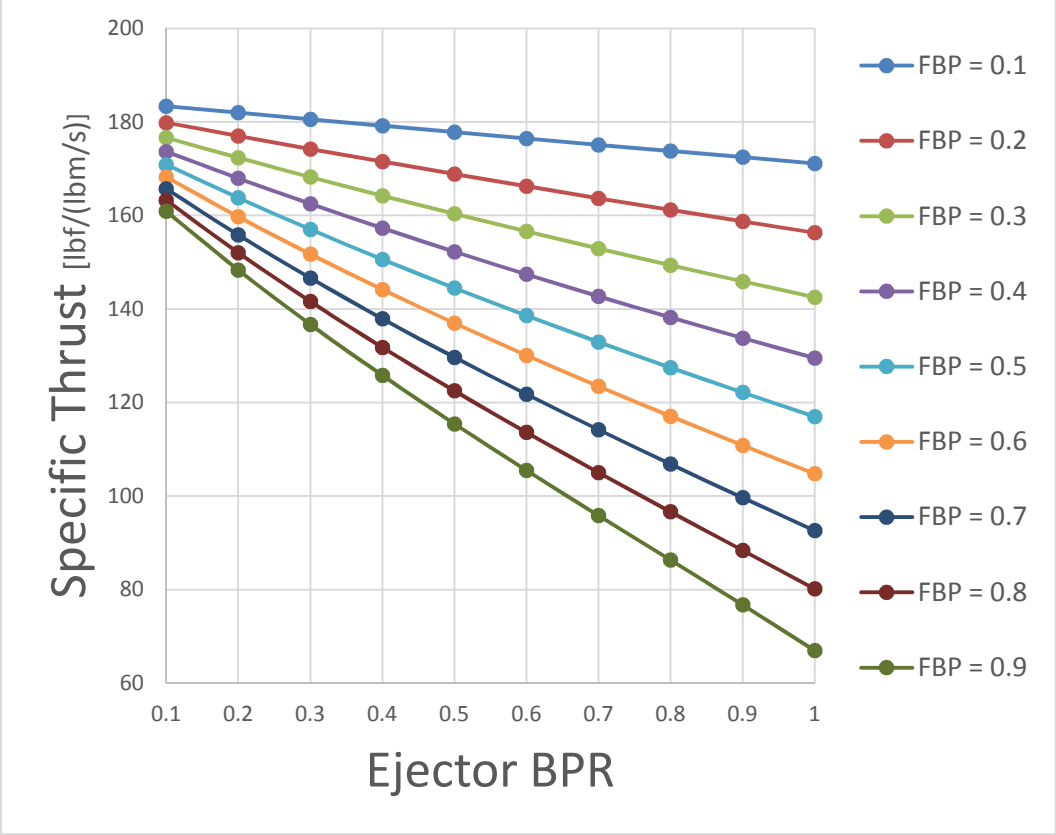

Figure 5-6: Variation of Specific Thrust as a function of Ejector Bypass Ratio at different Fan Bypass Ratios

In a low bypass ratio turbofan engine, the largest component in cross-sectional area is the nozzle.[23] This is especially the case in supersonic engines as there has to be a divergent section of the nozzle to exhaust the engine flow at supersonic speeds.[23]

In modern military fighter aircraft, the engines are no longer located on engine nacelles under the wing but inside the engine airframe due to various reasons including drag, reducing of heat signature and susceptibility to enemy fire [24], which has led to airframe interior space becoming a premium with emphasis on smaller, more efficient engines for payload and fuel.[25]

By keeping the nozzle exit area to a minimum, the overall volume occupied by the engine is reduced and leaves more space for weapons payload, avionics, fuel, etc.

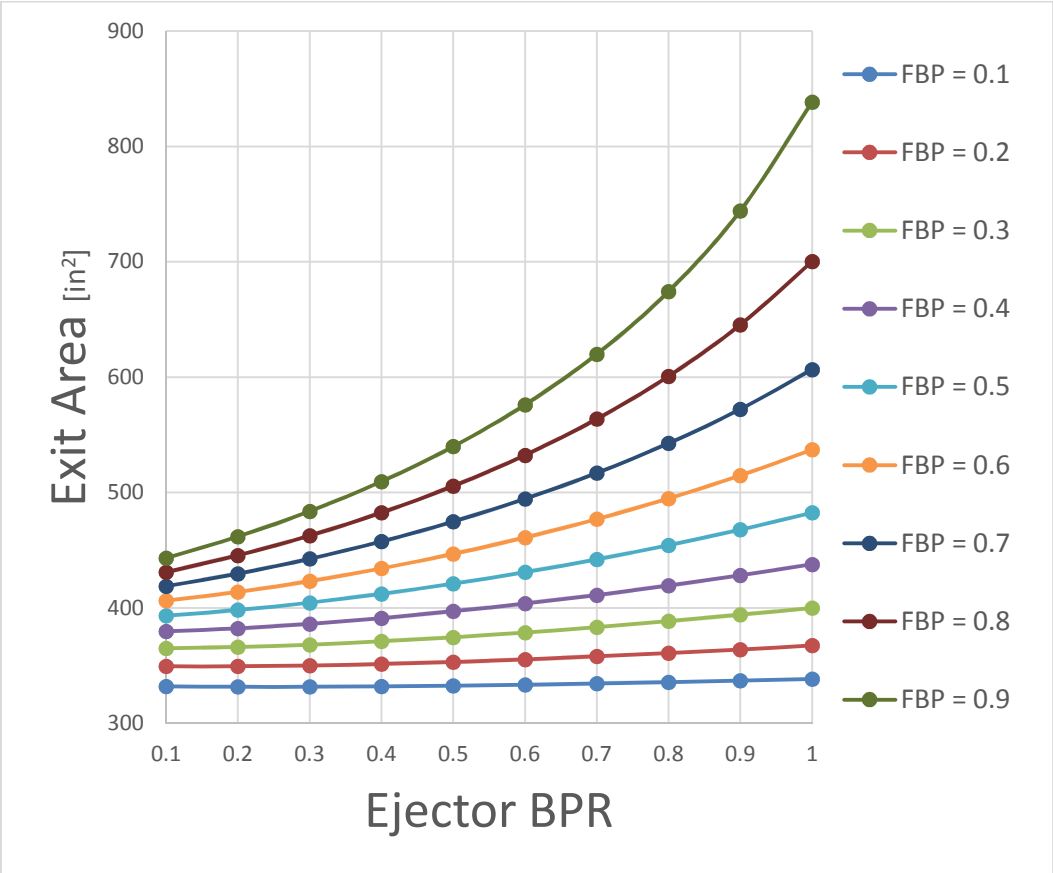

Figure 5-7: Variation of Nozzle Exit Area as a function of Ejector Bypass Ratio at different Fan Bypass Ratios

Figure 5-7 shows that lower bypass ratios result in smaller nozzle exit areas. This is due to the amount of mass flow rate at lower BPRs being less than at high BPRs resulting in the nozzle having to exhaust lower mass flow rates, resulting in a smaller nozzle.

Ejector nozzles have the advantage of exhausting the airflow at a colder exit static temperature which helps in suppression of noise.[26] Hence choosing an ejector bypass ratio that results in a lower static temperature exit is important.

In Figure 5-8, as the FBP increases, the exit static temperature increases for the same EBP. But for the same FBP, increase in EBP leads to drop in exit static temperature. Also at low FBP, the ejector nozzle provides extremely good noise suppression, leading to a quieter engine and stealthier aircraft.[27]

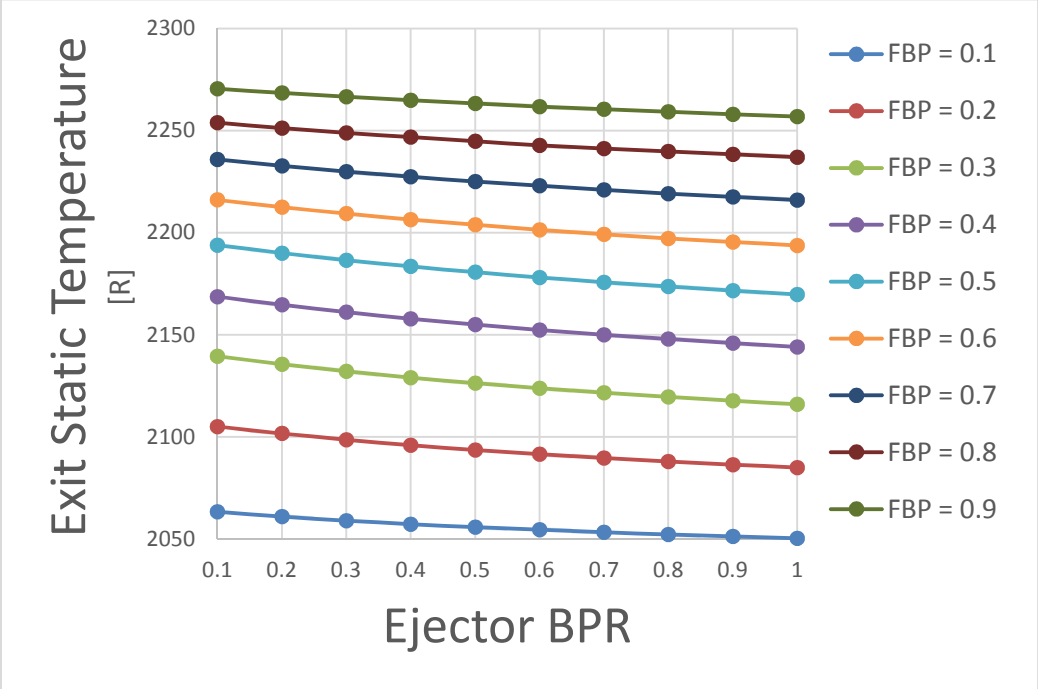

Figure 5-8: Variation of Exit Static Temperature as a function of Ejector Bypass Ratio at different Fan Bypass Ratios

By keeping the nozzle exit area low, the nozzle is smaller in diameter and hence lighter. This reduces the overall weight of the engine and improves the thrust-to-weight ratio. Low FBPs provide the best SFC and specific thrust, but increase the noise of the engine. But as the bypass ratios increase, the engine loses its performance drastically.

From Figures 5-2 through 5-8, at FBP = 0.1 and EBP = 0.5, the engine gives balanced performance. Hence a fan bypass ratio of 0.1 and an ejector bypass ratio of 0.5 is selected as the optimal bypass ratios for the ejector-nozzle turbofan engine for the defined mission envelope.

5.2 Comparative Analysis

The optimized ejector turbofan engine is then compared with three different engine configurations at off-design conditions to determine its advantages and disadvantages.

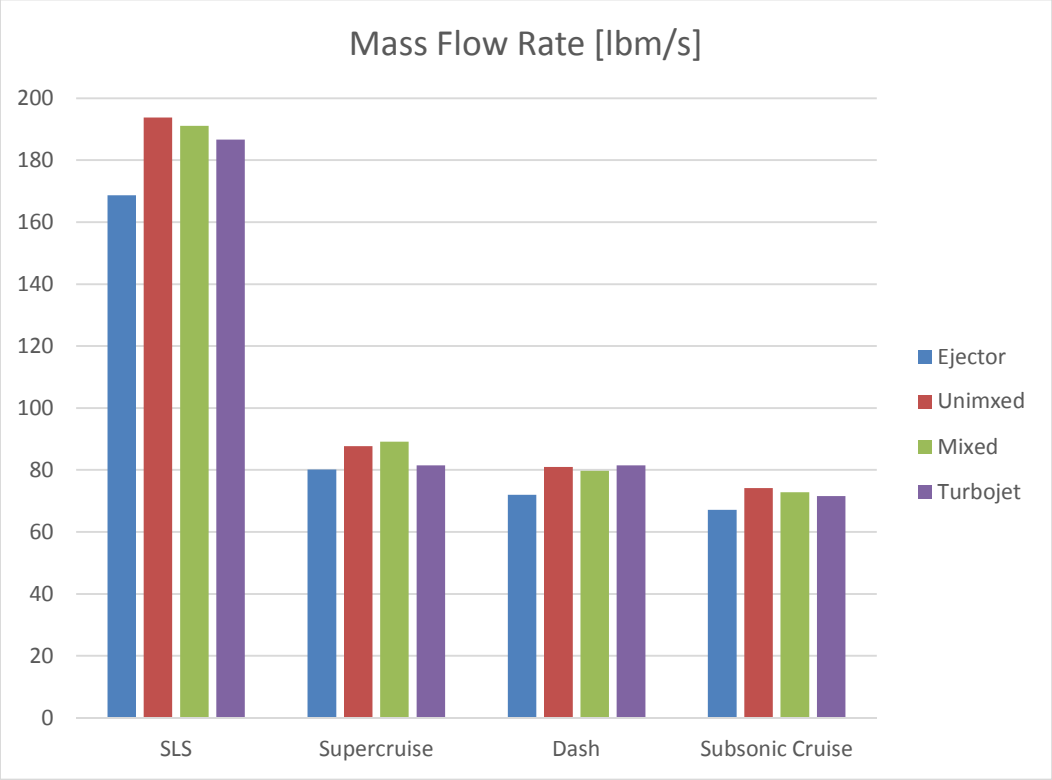

Figure 5-9: Mass Flow Rate (Comparative Analysis)

Mass flow rates for the ejector turbofan are the lowest across all off-design conditions. It is almost 15% lower at SLS when compared to the other engine configurations resulting in a less bulky engine.

As the mass flow rates of the ejector turbofan are lower when compared to the other engine models, the fuel flow rates also decreases. Figures 5-10 & 5-11 show that the fuel consumption of the ejector based turbofan is lesser compared to the other configurations.

Similar performance is also obtained at off-design conditions with the afterburner burning less fuel, increasing the range of the aircraft.

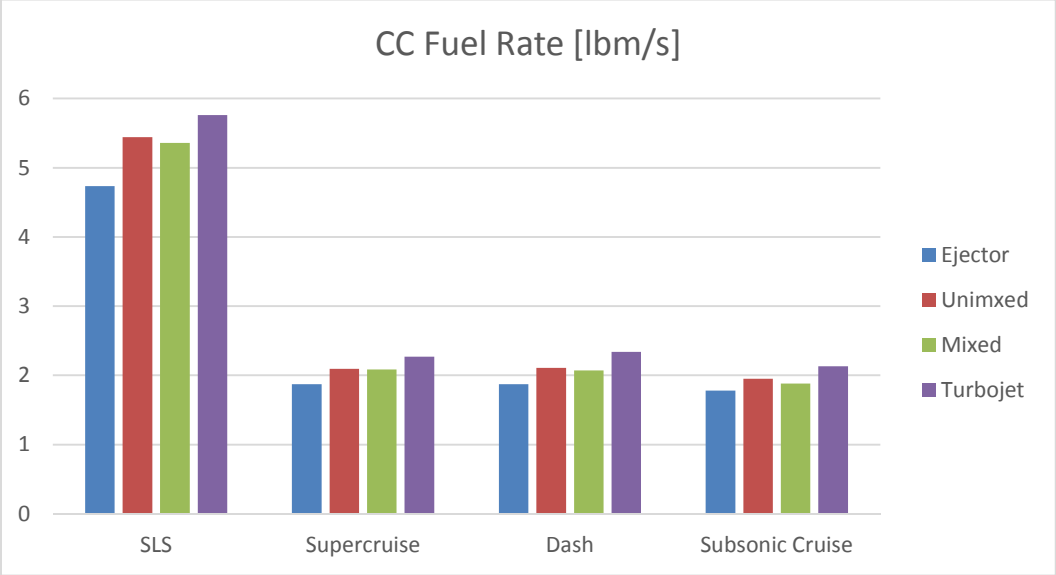

Figure 5-10: Combustion Chamber Fuel Flow Rate (Comparative Analysis)

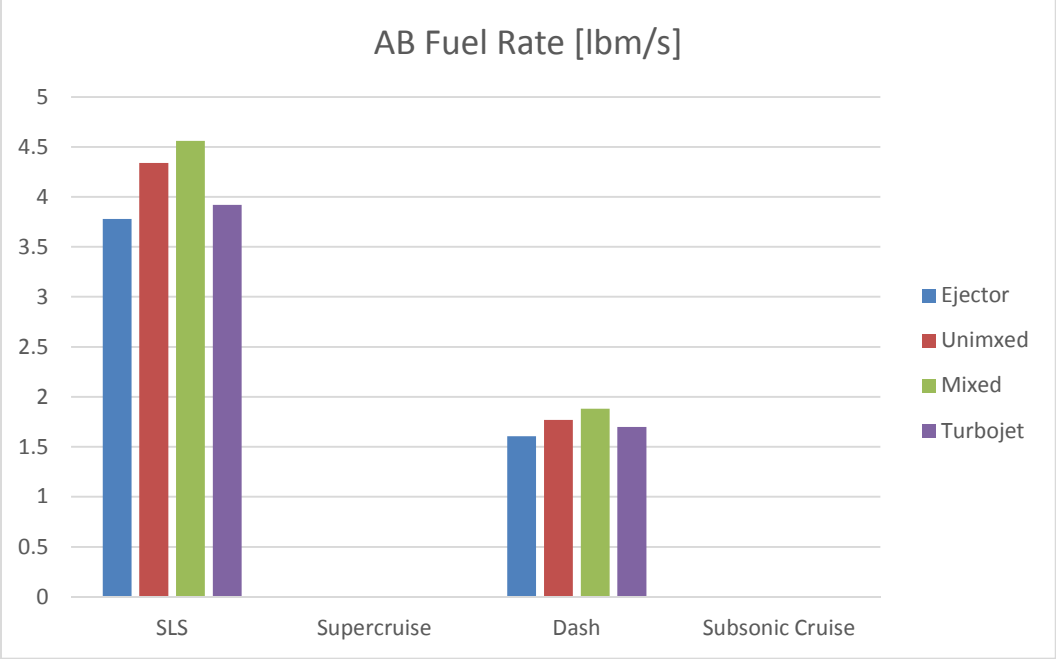

Figure 5-11: Afterburner Fuel Flow Rate (Comparative Analysis)

Gross thrust is the total thrust produced by the engine. It is a measure of the capability of the engine to produce the maximum thrust at the given operating conditions if the aircraft is stationary (resulting in zero inlet momentum flux loss).[15]

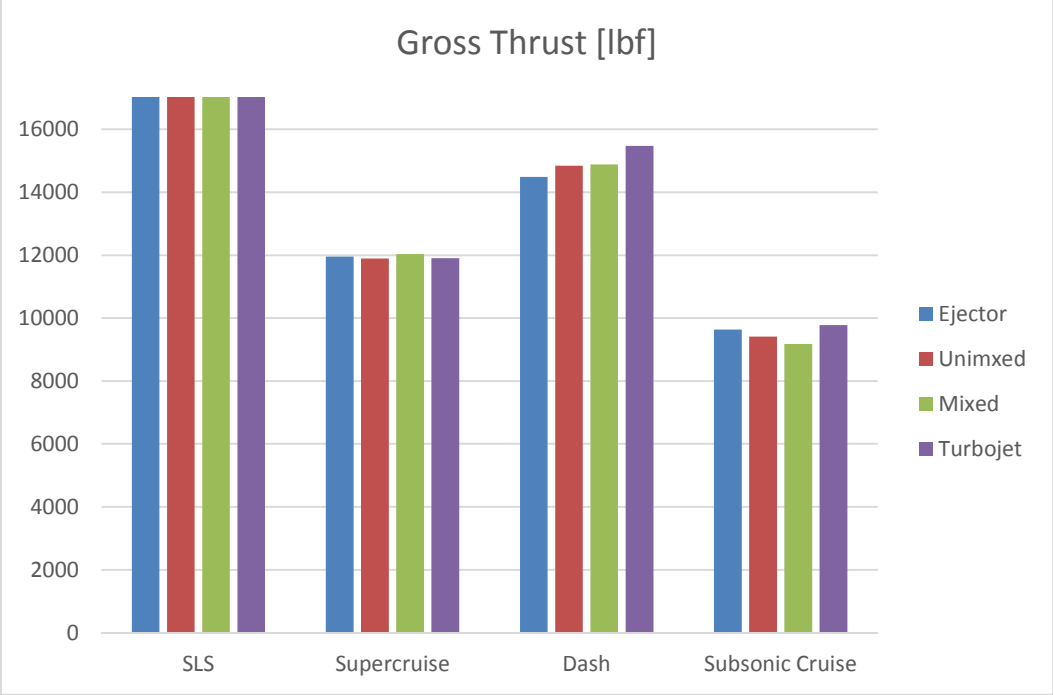

Figure 5-12: Gross Thrust (Comparative Analysis)

From Figure 5-12, we see that at supercruise condition, the ejector provides the about the same gross thrust, while at dash and subsonic cruise, its thrust level is slightly lower than the other engines.[11]

The net thrust is the gross thrust minus the ram drag which is the thrust that is delivered by the engine.[15] By calculating the net thrust for each engine at off-design conditions in terms of percentage of its gross thrust (Table 5-1), we find that even though the net thrust gained from the ejector turbofan is less than the other configurations at dash and subsonic cruise (Figure 5-13), it converts a higher percentage of thrust from the gross thrust to the net thrust which makes the ejector-nozzle turbofan more efficient in

off-design cases. The smaller area of the engine inlet reduces the ram drag. The net thrust of the ejector-nozzle turbofan is lower when compared to the other configurations due to the low mass flow rate.

Table 5-2: Net Thrust as %Gross Thrust at Off-Design Conditions

	Ejector	**Unmixed**	**Mixed**	**Turbojet**
Supercruise	67.71	64.51	64.31	67.03
Dash	70.09	67.16	67.74	68.27
Subsonic Cruise	82.17	79.86	79.69	81.29

As explained previously, the ejector provides maximum net thrust at Supercruise conditions but is not an improvement for dash and subsonic cruise.

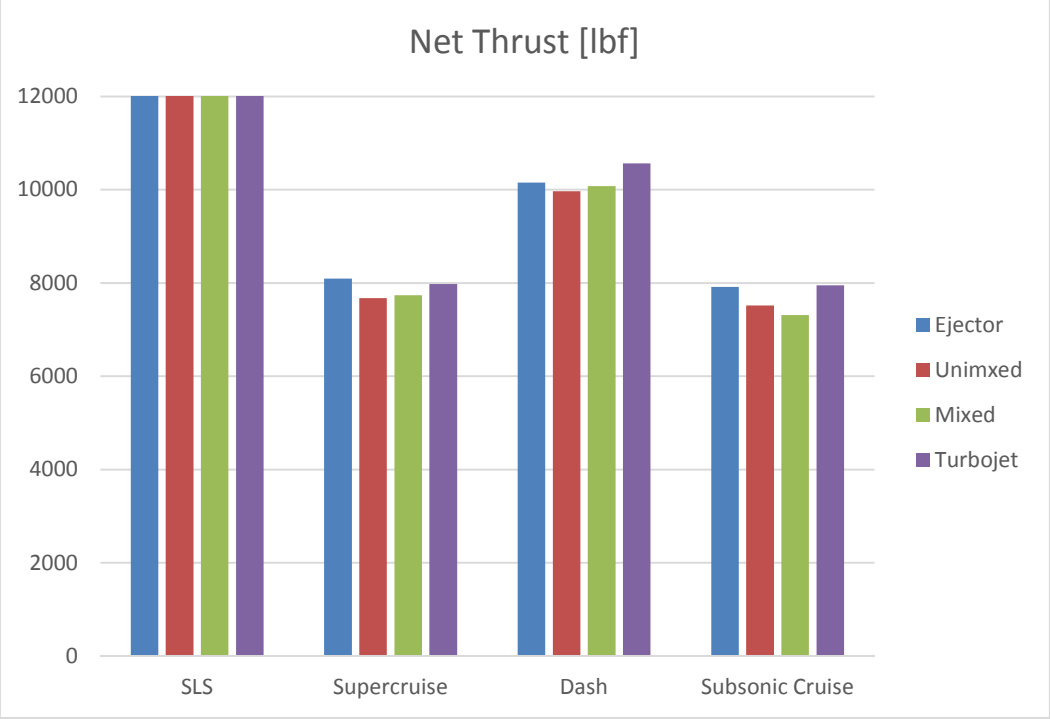

Figure 5-13: Net Thrust (Comparative Analysis)

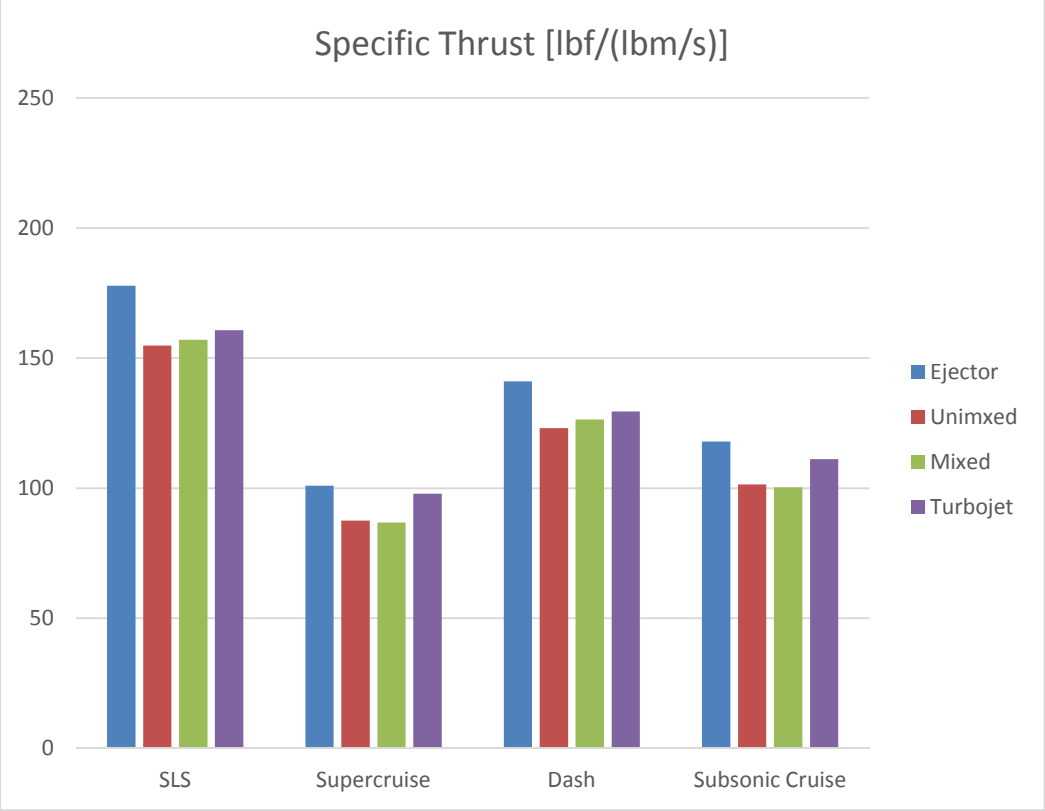

Figure 5-14: Specific Thrust (Comparative Analysis)

Figure 5-14 gives the specific thrust of the engines. The ejector-nozzle turbofan has a higher specific thrust than the other configurations due to its low mass flow rate and high thrust augmentation. At supercruise and dash conditions, there is a 15% difference in specific thrust of the ejector turbofan when compared to the other bypass engines with only the turbojet coming close at 3% difference, resulting in an engine that occupies less space, minimizing drag.

Similarly, the SFC of the ejector-nozzle turbofan is approximately 15% lower when compared to other engines (Figure 5-15), resulting in a highly efficient, less bulky, long range engine.

Figure 5-15: SFC (Comparative Analysis)

As the specific thrust increases, the nozzle exit area decreases.[20] This is apparent in Figure 5-16, where the nozzle exit area of the ejector turbofan is at least 12% lower when compared to the other engines.

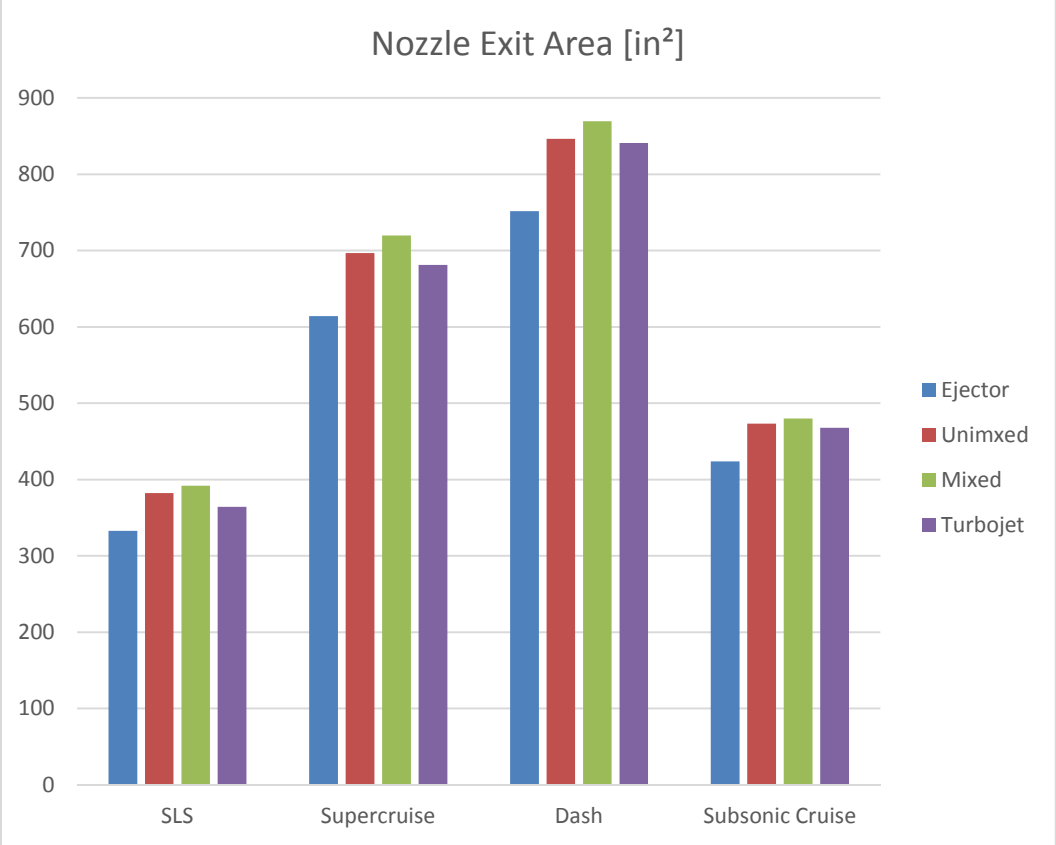

Figure 5-16: Nozzle Exit Area (Comparative Analysis)

From the above results, we find that ejector-based low bypass turbofan engines have low SFC, high specific thrust and low nozzle exit area causing them to be very small in diameter, highly efficient in design and performance at supercruise and on-par performance at dash and subsonic cruise.

CHAPTER 6

Conclusion

The results are summarized in this chapter and the implication of the research work is discussed. Further improvements on research methodology are also discussed.

6.1 Summary and Conclusion

The requirements of this research study were numerous. First, an ejector nozzle was to be designed for a low bypass turbofan engine using NPSS. This was done by designing a low bypass turbofan engine and using equations for a control volume approach to model the performance of the ejector nozzle. By ensuring that the primary nozzle expanded to the ambient pressure, the thermodynamic properties of the flow obtained through NPSS ensured that the working of the ejector nozzle could be modeled.

The second requirement was to develop a model for comparison of the turbofan engines. In the industry, for the development of military fighter aircraft, first a thrust requirement of the engine is decided before engine sizing is performed.[28] Therefore, in this research study, a thrust requirement of 30000 lbf was imposed on all trials which allowed for the simulation of the engine. This form of analysis allowed a large number of engines having different bypass parametric combinations to be studied from geometrical and efficiency standpoints.

Once the engine model was completed, operational parameters were varied to perform an optimization study. As optimized studies of pressure ratios have already been conducted [6,7], fan and ejector bypass ratios were varied in this research study. For a military aircraft, low bypass ratios are generally preferred, ranging from 0.1 to 1.0. Using these parameters, curves for mass flow rate, fuel flow rate, specific thrust, specific fuel consumption, nozzle exit static temperature and nozzle exit area were obtained. A fan

bypass ratio of 0.1 and ejector bypass ratio of 0.5 were found to be the most optimum bypass ratios for the given thrust requirements at sea-level-static on-design conditions.

To compare the performance of the ejector nozzle turbofan engine at off-design condition, a model flight envelope for military fighter aircrafts was designed involving three significant sections: supercruise, dash and subsonic cruise. In addition to the ejector nozzle engine, three conventional gas turbine engines were compared: Unmixed-flow low bypass, Mixed-flow low bypass turbofan engines and Turbojet engine. Thrust capabilities of each engine at off-design conditions were compared and it was found that though the ejector nozzle turbofan was equal or lower than the other configurations in terms of gross thrust, the percentage of gross thrust converted into net thrust was highest for the ejector turbofan. The specific thrust was 15% higher for the ejector nozzle turbofan when compared to the bypass flow engines and 6% higher for the turbojet engine. For specific fuel consumption, the ejector was 15% lower at supercruise and 12% lower for dash and subsonic cruise. The nozzle exit area for the ejector was 10-15% lower at all off-design conditions. These results show that a turbofan engine containing an ejector nozzle is much smaller in diameter but longer due to the length of the mixing chamber. Also it is more efficient than other conventionally configured engine configurations for the defined flight envelope.

From experimental studies, it is found that the advantages of using ejector nozzle includes better off-design performance, smaller engines and lower exit static temperature resulting in a quieter engine thereby making the aircraft more stealthy. From this simulation study, we see that the ejector nozzle does provide these advantages.

The NPSS model developed can be used to simulate the ejector nozzle for various on-design and off-design conditions. The advantage of using NPSS is the time taken for the calculation of each trial is drastically reduced. Also due to its object-oriented

structure, configurations can easily be modified as per the user's requirements. This allows for an easier test bed for obtaining analytical solutions of ejector nozzle analyses.

6.2 Improvements

A number of improvements can be made to this study to improve the scope of the research. The ejector model developed in this thesis uses a correction factor that accounts for loss in exit static temperature due to incomplete mixing. In addition to the correction factor, when one of the flows is supersonic, a portion of the secondary flow remains unmixed. This is approximated by a model called 'Fabri Choking' in which an inviscid slip line forms that behaves as a solid boundary causing the unmixed secondary flow to reach a maximum of Mach unity condition.[29]

In the development of the ejector model, a control volume approach is utilized. This is valid for a zero-D approach but fails to account for non-uniformity in velocity profiles and variation of thermodynamic properties in 2D and 3D analyses. Effect of boundary layer formation is neglected which causes a minor dip in performance. Momentum and convection losses are inaccurately modelled using arbitrary corrective terms.

Studies have been conducted to maximize mixing of flows in the shortest length possible. Increasing mixing surface area by having multiple primary nozzles, variable area mixing tubes [30], lobed nozzle contours [31], introducing vortices [32], etc. are some of the attempts made to promote mixing.

To tackle the aforementioned problems, a new method of ejector analysis must be devised. A separate element for ejector nozzles can be written in NPSS using the physical phenomena approach. A combination of viscid and inviscid analyses can be utilized in the physical phenomena approach by determining the velocity profile of the primary and secondary flows and calculating the boundary layer thickness.[33,34] The

region across which mixing occurs can be obtained using numerical techniques.[35] A comprehensive analysis can be performed to determine, for particular flight conditions, the best design of the ejector that allows for maximum mixing in the shortest length possible. A combination of such techniques would be useful in the optimization of thrust augmenting ejector nozzles.

Current techniques for predicting static and dynamic thrust performance must incorporate variable component losses to predict realistic performance. Transient analysis with capabilities for tertiary air flow for take-off and climb simulation can be incorporated into the NPSS model discussed in this study. Also a variety of flight conditions can be tested to get a complete picture of the performance of ejectors with respect to altitude and flight speed. Acoustic modeling can be conducted to study the effect of ejector nozzles on its surroundings.

In NPSS, the variable exit-area convergent-divergent nozzle changes its exit area to ensure that the flow expands to the ambient pressure. Though this takes place in modern engines, the extent to which the area is varied is physically constrained due to mechanical and aerodynamic reasons. Hence this constraint can be written into the code of the ejector nozzle to ensure that it stays within the physical capabilities of the engine and aircraft.

Due to the lack of high performance computing in the 1970s and 1980s, ejector analysis was done primarily by simple numerical techniques. With the advent of CFD, turbulence modelling of the ejector mixer can be done to further study the effect of engine parameters on the performance of the ejector nozzle.

Fundamental studies to define a comprehensive set of design data needs to be performed with a unified theory of the working of an ejector nozzle established. This will allow for a more widespread understanding of the physics inside a thrust augmenting

ejector nozzle and increased research with validation from computational and experimental results.

APPENDIX A

Results

A.1 SLS

SLS	Ejector-based	Unmixed	Premixed	Turbojet
Mass Flow Rate, $\dot{m}_0$, lbm/s	168.71	193.82	191.04	186.69
Compressor Pressure Ratio, π_c	36	36	36	36
Fan Pressure Ratio, π_f	5	5	5	5
HP Compressor Pressure Ratio, π_{ch}	7.2	7.2	7.2	7.2
Burner Fuel Flow Rate, lbm/sec	4.73	5.44	5.36	5.76
Afterburner Fuel Flow Rate, lbm/sec	3.78	4.34	4.56	3.92
Gross Thrust, lbf	30000	30000	30000	30000
Net Thrust, lbf	30000	30000	30000	30000
Specific Thrust, lbf/(lbm/s)	177.82	154.78	157.04	160.70
SFC, lbm/(hr*lbf)	1.0216	1.1737	1.1899	1.1621
Nozzle Exit Area, in^2	332.63	382.15	392.06	364.33
Nozzle Area Ratio	1.87	1.87	1.85	1.99
Exit Static Temperature, R	2055.74	2569.70	2582.51	2513.14
Exit Mach Number	2.58	2.03	2.02	2.10

A.2 Supercruise

Supercruise	Ejector-based	Unmixed	Premixed	Turbojet
Mass Flow Rate, $\dot{m}_0$, lbm/s	80.16	87.66	89.19	81.45
Compressor Pressure Ratio, π_c	30.13	29.64	29.84	31.05
Fan Pressure Ratio, π_f	5.76	5.87	5.84	6.93
HP Compressor Pressure Ratio, π_{ch}	5.23	5.05	5.11	4.48
Burner Fuel Flow Rate, lbm/sec	1.87	2.10	2.90	2.27
Afterburner Fuel Flow Rate, lbm/sec	0	0	0	0
Gross Thrust, lbf	11957.2	11896.6	12035.6	11899.6
Net Thrust, lbf	8096.54	7674.65	7739.83	7976.67
Specific Thrust, lbf/(lbm/s)	101.00	87.55	86.78	97.93
SFC, lbm/(hr*lbf)	0.8322	0.9827	0.9702	1.0254
Nozzle Exit Area, in^2	614.21	696.74	719.87	681.37
Nozzle Area Ratio	3.45	3.41	3.39	3.72
Exit Static Temperature, R	905.03	1137.44	1095.69	1218.83
Exit Mach Number	2.24	2.67	2.65	2.72

A.3 Dash

Dash	Ejector-based	Unmixed	Premixed	Turbojet
Mass Flow Rate, $\dot{m}_0$, lbm/s	71.98	80.95	79.74	81.54
Compressor Pressure Ratio, π_c	16.82	16.57	16.57	16.90
Fan Pressure Ratio, π_f	2.88	2.97	2.99	2.77
HP Compressor Pressure Ratio, π_{ch}	5.84	5.58	5.54	6.10
Burner Fuel Flow Rate, lbm/sec	1.87	2.11	2.07	2.34
Afterburner Fuel Flow Rate, lbm/sec	1.61	1.77	1.88	1.70
Gross Thrust, lbf	14486.7	14840.2	14880.2	15473.4
Net Thrust, lbf	10153.10	9966.96	10079.8	10564.3
Specific Thrust, lbf/(lbm/s)	141.05	123.13	126.42	129.56
SFC, lbm/(hr*lbf)	1.2329	1.4011	1.4108	1.3758
Nozzle Exit Area, in^2	751.69	846.20	869.57	840.87
Nozzle Exit Area Ratio	4.23	4.14	4.09	4.59
Exit Static Temperature, R	1540.75	1939.68	1947.21	1872.34
Exit Mach Number	2.37	2.75	2.75	2.85

A.4 Subsonic Cruise

Subsonic Cruise	Ejector-based	Unmixed	Premixed	Turbojet
Mass Flow Rate, $\dot{m}_0$, lbm/s	67.11	74.12	72.86	71.55
Compressor Pressure Ratio, π_c	46.51	43.87	43.01	45.12
Fan Pressure Ratio, π_f	8.91	8.17	8.04	8.34
HP Compressor Pressure Ratio, π_{ch}	5.22	5.37	5.35	5.41
Burner Fuel Flow Rate, lbm/sec	1.78	1.95	1.88	2.13
Afterburner Fuel Flow Rate, lbm/sec	0	0	0	0
Gross Thrust, lbf	9632.32	9416.00	9176.38	9782.62
Net Thrust, lbf	7915.15	7519.47	7312.29	7951.83
Specific Thrust, lbf/(lbm/s)	117.94	101.45	100.37	111.13
SFC, lbm/(hr*lbf)	0.8095	0.9312	0.9256	0.9621
Nozzle Exit Area, in^2	423.88	473.25	480.013	467.75
Nozzle Exit Area Ratio	2.38	2.32	2.26	2.55
Exit Static Temperature, R	1027.75	1369.45	1333.68	1425.54
Exit Mach Number	2.37	2.28	2.25	2.36

APPENDIX B

NPSS Output for Optimized Ejector-Nozzle Turbofan Engine at On-Design Conditions

```
========================================
=====    RUNNING DESIGN POINT     =====
========================================


Solver Indep and Dep variables

{"ind_Wair",
"ind_Wfuel",
"ind_Wfuel2",
"TrbH.S_map.ind_PRbase",
"TrbL.S_map.ind_PRbase" }

{"dep_Fn",
"dep_T4",
"dep_T7",
"ShH.integrate_Nmech",
"ShL.integrate_Nmech" }

Altitude = 0 ft
Mach Number = 0
Engine Air Flow = 168.714 lbm/s

F000 Tt = 518.67 R
F000 Ts = 518.67 R
F020 Tt = 518.67 R
F030 Tt = 1567.06 R
F040 Tt = 3600.02 R
F045 Tt = 3047.86 R
F050 Tt = 2757.28 R
```

F070 Tt = 4000.02 R

F090 Tt = 3850.82 R

F090 Ts = 2055.74 R

F275 Tt = 866.647 R

F000 Pt = 14.6959 psia

F000 Ps = 14.6959 psia

F020 Pt = 14.1081 psia

F030 Pt = 507.891 psia

F040 Pt = 507.891 psia

F045 Pt = 215.512 psia

F050 Pt = 129.793 psia

F070 Pt = 123.136 psia

F070 Pt = 123.136 psia

F090 Pt = 119.442 psia

F090 Ps = 14.6959 psia

Fan Splitter BPR = 0.1

Ejector Splitter BPR = 0.5

CompF PR = 5

CompF Adiab eff = 0.863075

CompF Poly eff = 0.889761

CompF Pwr = -20084 hp

CompH PR = 7.2

CompH Adiab eff = 0.8695

CompH Poly eff = 0.898333

CompH Pwr = -38816.2 hp

TurbH PR = 2.35668

TurbH Adiab eff = 0.89895

TurbH Poly eff = 0.890139

TurbH Pwr = 38812.4 hp

TurbL PR = 1.66043

TurbL Adiab eff = 0.89595

TurbL Poly eff = 0.890636

TurbL Pwr = 20084.5 hp

Shaft L RPM = 8000

Shaft H RPM = 16500

Secondary Nozzle Throat Area = 177.799 in2

Secondary Nozzle Exit Area = 332.632 in2

Secondary Nozzle Area Ratio = 1.87083

Wfuel = 4.73348 lbm/s

FAR = 0.0308619

Wfuel (AB) = 3.78011 lbm/s

FAR (AB) = 0.0520387

Total Wfuel = 30648.9 lbm/hr

SFC = 1.02162 lbm/(hr*lbf)

Specific Impulse = 3523.83 seconds

Gross Thrust = 30000.4 lbf

Net Thrust = 30000.4 lbf

Specific Thrust = 177.819 lbf/(lbm/s)

Acoustic Velocity = 2107.93

Exit Mach Number = 2.58372

Nozzle Exit Velocity = 5446.31 ft/s

Thrust Augmentation Ratio = 1.16234

Solver converged (1 = yes, 0 = no) ? = 1

Iterations = 11

Constraints Active? = 0

Constraints Hit =

==========

===== RUNNING OFF DESIGN POINT (SUPERCRUISE) =====

==========

Solver Indep and Dep variables

{"CmpFSec.S_map.ind_RlineMap",
"CmpH.S_map.ind_RlineMap",
"FsEng.ind_W",
"ind_Wfuel",
"ShH.ind_Nmech",
"ShL.ind_Nmech",
"SpltFan.ind_BPR",
"TrbH.S_map.ind_PRbase",
"TrbL.S_map.ind_PRbase" }

{"CmpFSec.S_map.dep_errWc",
"CmpH.S_map.dep_errWc",
"dep_T4",
"MixAConst.dep_errPs",
"NozSec.dep_Area",
"ShH.integrate_Nmech",
"ShL.integrate_Nmech",
"TrbH.S_map.dep_errWp",
"TrbL.S_map.dep_errWp" }

Altitude = 49212.6 ft
Mach Number = 1.6
Engine Air Flow = 80.1601 lbm/s

F000 Tt = 590.071 R

F000 Ts = 389.97 R

F020 Tt = 590.07 R

F030 Tt = 1708.31 R

F040 Tt = 3600 R

F045 Tt = 3068.79 R

F050 Tt = 2628.51 R

F070 Tt = 2456.44 R

F090 Tt = 2389.5 R

F090 Ts = 905.032 R

F275 Tt = 1050.87 R

F000 Pt = 7.42755 psia

F000 Ps = 1.74688 psia

F020 Pt = 7.13045 psia

F030 Pt = 214.853 psia

F040 Pt = 214.853 psia

F045 Pt = 94.5436 psia

F050 Pt = 43.4216 psia

F070 Pt = 42.6486 psia

F070 Pt = 42.6486 psia

F090 Pt = 41.3692 psia

F090 Ps = 1.74687 psia

Fan Splitter BPR = 0.1

Ejector Splitter BPR = 0.5

CompF PR = 5.76131

CompF Adiab eff = 0.814478

CompF Poly eff = 0.852988

CompF Pwr = -12768.4 hp

CompH PR = 5.23001

CompH Adiab eff = 0.876389

CompH Poly eff = 0.899385

CompH Pwr = -15711.1 hp

TurbH PR = 2.27252

TurbH Adiab eff = 0.897021

TurbH Poly eff = 0.888434

TurbH Pwr = 15711.1 hp

TurbL PR = 2.17734

TurbL Adiab eff = 0.899948

TurbL Poly eff = 0.891668

TurbL Pwr = 12768.4 hp

Shaft L RPM = 9203.82

Shaft H RPM = 17308

Secondary Nozzle Throat Area = 177.799 in2

Secondary Nozzle Exit Area = 614.213 in2

Secondary Nozzle Area Ratio = 3.45453

Wfuel = 1.87162 lbm/s

FAR = 0.0288505

Wfuel (AB) = 0 lbm/s

FAR (AB) = 0.0249335

Total Wfuel = 6737.84 lbm/hr

SFC = 0.832188 lbm/(hr*lbf)

Specific Impulse = 4325.95 seconds

Gross Thrust = 11957.2 lbf

Net Thrust = 8096.54 lbf

Specific Thrust = 101.005 lbf/(lbm/s)

Acoustic Velocity = 1420

Exit Mach Number = 2.23633

Nozzle Exit Velocity = 3175.58 ft/s

Thrust Augmentation Ratio = 1.24835

Solver converged (1 = yes, 0 = no) ? = 1

Iterations = 31

Constraints Active? = 0

Constraints Hit =

==========

===== RUNNING OFF DESIGN POINT (DASH) =====

==========

Solver Indep and Dep variables

{"CmpFSec.S_map.ind_RlineMap",
"CmpH.S_map.ind_RlineMap",
"FsEng.ind_W",
"ind_Wfuel",
"ind_Wfuel2",
"ShH.ind_Nmech",
"ShL.ind_Nmech",
"SpltFan.ind_BPR",
"TrbH.S_map.ind_PRbase",
"TrbL.S_map.ind_PRbase" }

{"CmpFSec.S_map.dep_errWc",
"CmpH.S_map.dep_errWc",
"dep_T4",
"dep_T7",
"MixAConst.dep_errPs",
"NozSec.dep_Area",
"ShH.integrate_Nmech",
"ShL.integrate_Nmech",
"TrbH.S_map.dep_errWp",
"TrbL.S_map.dep_errWp" }

Altitude = 49212.6 ft

Mach Number = 2

Engine Air Flow = 71.9841 lbm/s

F000 Tt = 702.049 R

F000 Ts = 389.969 R

F020 Tt = 702.046 R

F030 Tt = 1746.21 R

F040 Tt = 3600 R

F045 Tt = 3028.13 R

F050 Tt = 2741.53 R

F070 Tt = 4000 R

F090 Tt = 3859.1 R

F090 Ts = 1540.75 R

F275 Tt = 1041.14 R

F000 Pt = 13.6756 psia

F000 Ps = 1.74686 psia

F020 Pt = 12.9918 psia

F030 Pt = 218.962 psia

F040 Pt = 218.962 psia

F045 Pt = 90.2012 psia

F050 Pt = 53.9936 psia

F070 Pt = 52.5653 psia

F070 Pt = 52.5653 psia

F090 Pt = 50.9884 psia

F090 Ps = 1.74687 psia

Fan Splitter BPR = 0.1

Ejector Splitter BPR = 0.5

CompF PR = 2.88483

CompF Adiab eff = 0.714047

CompF Poly eff = 0.752073

CompF Pwr = -8471.43 hp

CompH PR = 5.84223

CompH Adiab eff = 0.876289

CompH Poly eff = 0.900559

CompH Pwr = -17196.3 hp

TurbH PR = 2.42748

TurbH Adiab eff = 0.898618

TurbH Poly eff = 0.889397

TurbH Pwr = 17196.3 hp

TurbL PR = 1.67059

TurbL Adiab eff = 0.875098

TurbL Poly eff = 0.868691

TurbL Pwr = 8471.43 hp

Shaft L RPM = 6671.42

Shaft H RPM = 17582.2

Secondary Nozzle Throat Area = 177.799 in2

Secondary Nozzle Exit Area = 751.686 in2

Secondary Nozzle Area Ratio = 4.22773

Wfuel = 1.87122 lbm/s

FAR = 0.028306

Wfuel (AB) = 1.60615 lbm/s

FAR (AB) = 0.049659

Total Wfuel = 12518.5 lbm/hr

SFC = 1.23298 lbm/(hr*lbf)

Specific Impulse = 2919.76 seconds

Gross Thrust = 14486.7 lbf

Net Thrust = 10153.1 lbf

Specific Thrust = 141.046 lbf/(lbm/s)

Acoustic Velocity = 1825.88

Exit Mach Number = 2.37086

Nozzle Exit Velocity = 4328.9 ft/s

Thrust Augmentation Ratio = 1.15372

Solver converged (1 = yes, 0 = no) ? = 1

Iterations = 25

Constraints Active? = 0

Constraints Hit =

```
============================================================
=====  RUNNING OFF DESIGN POINT (SUBSONIC CRUISE)  =====
============================================================


Solver Indep and Dep variables

{"CmpFSec.S_map.ind_RlineMap",
"CmpH.S_map.ind_RlineMap",
"FsEng.ind_W",
"ind_Wfuel",
"ShH.ind_Nmech",
"ShL.ind_Nmech",
"SpltFan.ind_BPR",
"TrbH.S_map.ind_PRbase",
"TrbL.S_map.ind_PRbase" }

{"CmpFSec.S_map.dep_errWc",
"CmpH.S_map.dep_errWc",
"dep_T4",
"MixAConst.dep_errPs",
"NozSec.dep_Area",
"ShH.integrate_Nmech",
"ShL.integrate_Nmech",
"TrbH.S_map.dep_errWp",
"TrbL.S_map.dep_errWp" }

Altitude = 39370 ft
Mach Number = 0.85
Engine Air Flow = 67.1129 lbm/s
```

F000 Tt = 446.506 R

F000 Ts = 389.97 R

F020 Tt = 446.506 R

F030 Tt = 1671.68 R

F040 Tt = 3599.98 R

F045 Tt = 3082.38 R

F050 Tt = 2587.65 R

F070 Tt = 2515.09 R

F090 Tt = 2444.26 R

F090 Ts = 1088.86 R

F275 Tt = 1027.75 R

F000 Pt = 4.49748 psia

F000 Ps = 2.80361 psia

F020 Pt = 4.31758 psia

F030 Pt = 200.653 psia

F040 Pt = 200.653 psia

F045 Pt = 90.2204 psia

F050 Pt = 37.4509 psia

F070 Pt = 37.4533 psia

F070 Pt = 37.4533 psia

F090 Pt = 36.3297 psia

F090 Ps = 2.8036 psia

Fan Splitter BPR = 0.1

Ejector Splitter BPR = 0.5

CompF PR = 8.91233

CompF Adiab eff = 0.65846

CompF Poly eff = 0.74231

CompF Pwr = -13410.2 hp

CompH PR = 5.21451

CompH Adiab eff = 0.876923

CompH Poly eff = 0.899933

CompH Pwr = -14322.5 hp

TurbH PR = 2.22403

TurbH Adiab eff = 0.896622

TurbH Poly eff = 0.888237

TurbH Pwr = 14323 hp

TurbL PR = 2.40903

TurbL Adiab eff = 0.900785

TurbL Poly eff = 0.891625

TurbL Pwr = 13410.1 hp

Shaft L RPM = 12892.2

Shaft H RPM = 17068.9

Secondary Nozzle Throat Area = 177.799 in2

Secondary Nozzle Exit Area = 423.881 in2

Secondary Nozzle Area Ratio = 2.38405

Wfuel = 1.77986 lbm/s

FAR = 0.0293746

Wfuel (AB) = 0 lbm/s

FAR (AB) = 0.0274082

Total Wfuel = 6407.51 lbm/hr

SFC = 0.809525 lbm/(hr*lbf)

Specific Impulse = 4447.05 seconds

Gross Thrust = 9632.32 lbf

Net Thrust = 7915.15 lbf

Specific Thrust = 117.938 lbf/(lbm/s)

Acoustic Velocity = 1555.79

Exit Mach Number = 2.37597

Nozzle Exit Velocity = 3696.5 ft/s

Thrust Augmentation Ratio = 1.17528

Solver converged (1 = yes, 0 = no) ? = 1

Iterations = 67

Constraints Active? = 0

Constraints Hit =

References

[1] Shillito, T. B., Hearth, D. P., and Edgar M Cortright, J.," Exhaust Nozzles for Supersonic Flight with Turbojet Engines," NACA-RM-E56A18, April 1956.

[2] Porter, J. L., and R. A. Squyers, "A Summary/Overview of Ejector Augmentor Theory and Performance: Phase II (Technical Report) Volume I - Technical Discussion," Vought Corporation Advanced Technology Center, ATC-R-91100/9CR-47A, Dallas, TX, September 1979.

[3] Karman, T. von, “Theoretical Remarks on Thrust Augmentation,” *Reissner Anniversary Volume: Contribution to Applied Mechanics*, 1st ed., JW Edwards, Ann Arbor, 1949, pp. 461–468.

[4] Kochendorfer, F. D., and Rousso, M. D., "Performance Characteristics of Aircraft Cooling Ejectors Having Short Cylindrical Shrouds," NACA RM-E51E01, 1951.

[5] Heiser, W. H., “Thrust Augmentation,” Journal of Engineering for Power, vol. 89, 1967, PP. 75-82.

[6] Dutton, J. C., and Carroll, B. F., “Optimal Supersonic Ejector Designs,” *Journal of Fluid Engineering*, vol. 108, 1986, pp. 414–420.

[7] Chow, W. L., and Addy, A. L., “Interaction between Primary and Secondary Streams of Supersonic Ejector Systems and Their Performance Characteristics,” *AIAA Journal*, vol. 2, 1964, pp. 686–695.

[8] Fabri, J., and Paulon, J., “Theory and Experiments on Supersoinc Air-to-Air Ejectors,” NACA TM-1410, September 1958.

[9] Huang, K. P., and E. Kisielowski, "An Investigation of the Thrust Augmentation Characteristics of Jet Ejectors," Dynasciences Corp., DCR-219, Blue Bell, PA, April 1967.

[10] J. K. Johnson, J., Shumpert, P. K., and Sutton, J. F., "Steady Flow Ejector Research Program," Locheed-Georgia Company, ER-5332, Marietta, GA, September 1961.

[11] Heiser, W. H., “Ejector Thrust Augmentation,” *Journal of Propulsion and Power*, vol. 26, Nov. 2010, pp. 1325–1330.

[12] Gates, M. F., and Cochran, C. L., "Annular Nozzle Ejector, Phase II," Hiller Aircraft Corp. ARD-285, Firebaugh, CA, July 1961.

[13] Gates, M. F., and Fairbanks, J. W., "Annular Nozzle Ejector, Phase III," Hiller Aircraft Corp. ARD-300, Firebaugh, CA, July 1962.

[14] Jones, S., “Steady-State Modeling of Gas Turbine Engines Using The Numerical Propulsion System Simulation Code,” *ASME Turbo Expo 2010: Power for Land, Sea and Air*, ASME, Glasgow, UK, 2010, pp. 1–28.

[15] Mattingly, J. D., and Ohain, H. von, "Elements of Propulsion: Gas Turbines and Rockets," AIAA, Virginia, 2006.

[16] Mattingly, J. D., Heiser, W. H., and Pratt, D. T., "Aircraft Engine Design," AIAA, Virginia, 2002.

[17] Keenan, J. H., Neumann, E. P., and Lustwerk, F., “An Investigation of Ejector Design by Analysis and Experiment,” *Journal of Applied Mechanics*, vol. 17, 1950, pp. 299–309.

[18] Hemighaus, G., Boval, T., and Bacha, J., "Aviation Fuel Technical Review," Chevron Corp., FTR-3, Houston, TX, October 2014.

[19] Jack L. Kerrebrock, "Typical Axial Flow Engine Compressor and Turbine Characteristivs at Maximum Power," *Aircraft Engines & Gas Turbines*, 2nd ed., The MIT Press, Cambridge, MA, April 1992.

[20] Georgiadis, N. J., Dalbello, T. W., Trefny, C. J., and Johns, A. L., “Aerodynamic Design and Analysis of High Performance Nozzles for Mach 4 Accelerator Vehicles,” AIAA Paper, 2006-0016, January 2006, pp. 1–14.

[21] Oates, G. C., "Aerothermodynamics of Gas Turbine and Rocket Propulsion," AIAA, Virginia, 1997.

[22] Oates, G. C., "Aircraft Propulsion Systems Technology and Design," AIAA, Virginia, 1989.

[23] Oates, G. C., "Aerothermodynamics of Aircraft Engine Components," AIAA, Virginia, 1985.

[24] Anderson, J. D., "Fundamentals of Aerodynamics," McGraw-Hill, NY, 2001.

[25] Hünecke, K., "Jet Engines: Fundamentals of Theory, Design and Operation," Zenith Press, US, 2005.

[26] Mcclintock, F. A., and Hoodt, J. H., “Aircraft Ejector Performance,” *Journal of the Aeronautical Sciences*, vol. 13, 1946, pp. 559–568.

[27] Hendricks, E. S., and Seidel, J. A., “A Multidisciplinary Approach to Mixer-Ejector Analysis and Design,” NASA TM-2012-217709, September 2012.

[28] Gunston, B., "Jane’s Aero-Engines 2014/2015," Jane’s Information Group, Englewood, CO, 2014.

[29] Ahren, B., “Analysis of Ejectors Used as Supersonic Propelling Nozzles for Jet Engines,” Ph.D Dissertation, Departyment of Aeronautical and Vehicle Engineering, KTH Royal Institute of Technology, Sweden, 1968.

[30] Hickman, K. E., Hill, P. G., and Gilbert, G. B., “Analysis and Testing of Compressible Flow Ejectors With Variable Area Mixing Tubes,” *Journal of Basic Engineering*, vol. 94, Jun. 1972, p. 407.

[31] Tillman, T. G., Paterson, R. W., and Presz, W. M., “Supersonic Nozzle Mixer Ejector,” *Journal of Propulsion and Power*, vol. 8, 1992, pp. 513–519.

[32] Tillman, T. G., and Presz, W. M., “Thrust Characteristics of a Supersonic Mixer Ejector,” *Journal of Propulsion and Power*, vol. 11, 1995, pp. 931–937.

[33] Weber, H. E., “Ejector-Nozzle Flow and Thrust,” *Journal of Fluids Engineering*, vol. 82, Mar. 1960, pp. 120–129.

[34] Weber, H. E., “Ejector-Nozzle Flow and Thrust for Choked Flow,” *Journal of Fluids Engineering*, vol. 83, Sep. 1961, pp. 471–477.

[35] Hewedy, N. I. I., Hamed, M. H., Abou-Taleb, F. S., and Ghonim, T. A., “Optimal Performance and Geometry of Supersonic Ejector,” J*ournal of Fluids Engineering*, vol. 130, 2008, pp. 1–10.

[36] "NPSS User Guide Reference Sheets", Wolverine Ventures, Florida, 2012.

Biographical Information

Hatim Soeb Rangwala earned his Bachelor of Engineering degree in Mechanical Engineering from Anna University, India in 2013. An avid tinkerer, he has worked on many small-scale projects like high-efficiency low input heat exchangers, self-recharging bicycles, lightweight aircrafts, etc., showcasing these projects at national engineering symposiums. In his junior and senior year, his focus shifted to design and simulation of aerospace technology. Certified in Solidworks and Ansys-Fluent, he used these tools to study the aerodynamics of various wing structures at different flight conditions and performed cold flow simulation of rocket engines using CFD. His aptitude for gas dynamics and CFD led him to pursue his Master of Science in Aerospace Engineering, specializing in propulsion and subsequent induction to the Aerodynamics Research Center (ARC) at The University of Texas at Arlington.

He has worked on thrust-augmenting ejector nozzles for his master's research. For his doctoral degree, the research goal is to conduct experiments on propulsive applications for ejectors with the end goal of developing a unified code to simulate all types of propulsive nozzles using Numerical Propulsion System Simulation software.